Food Research International 162 (2022) 111914

Contents lists available at ScienceDirect

Food Research International

journal homepage: www.elsevier.com/locate/foodres

Pectin-based color indicator films incorporated with spray-dried Hibiscus extract microparticles

Juliana Farinassi Mendes [a,*], Laís Bruno Norcino [b], Anny Manrich [a], Tiago José Pires de Oliveira [c], Rafael Farinassi Mendes [c], Luiz Henrique Capparelli Mattoso [a]

[a] National Laboratory of Nanotechnology for Agriculture (LNNA), Embrapa Instrumentation, São Carlos 13560-970, SP, Brazil
[b] Graduate Program in Biomaterials Engineering, Federal University of Lavras, Lavras 37200-000, MG, Brazil
[c] Department of Engineering, Federal University of Lavras, Lavras 37200-000, MG, Brazil

ARTICLE INFO

Keywords:
Intelligent packaging
Encapsulation
Biopolymer films
Continuous casting

ABSTRACT

Colorimetric films incorporated with anthocyanins as an indicator for freshness monitoring have aroused growing interest recently. The pH-sensing colorimetric film were developed based on pectin (HM), containing aqueous hibiscus extract microparticles (HAE). HAE microparticles were obtained by spray drying with different wall materials (Inulin -IN, maltodextrin- MD and their combination). The films were obtained on large scale by continuous casting. These films were characterized for physicochemical analysis, morphological structure, thermal and barrier properties, antioxidant activity, and color change at different pH. The addition of HAE microparticles caused relevant changes to HM-based films, such as in mechanical behavior and improved barrier property (11–22% WVTR reduction) depending on the type of wall material used and the concentration added. It was verified with the thermal stability of films, with a slight increase being observed. The color variation of smart films was entirely pH-dependent. Overall, the proposed color indicator films showed unique features and functionalities and could be used as an alternative natural pH indicator in smart packaging systems.

1. Introduction

In recent years, the development of active and intelligent packaging based on biopolymeric and biodegradable materials has been gaining emphasis in the scientific scenario (Agarwal, 2021; Jamróz et al., 2022; Priyadarshi, Roy, Ghosh, Biswas, & Rhim, 2021). Biodegradable intelligent packaging can be explored as freshness indicators of food, as capable of monitoring and informing the direct quality information of food products to consumers by responding to the changes occurring in products arose from microbial growth or metabolism (Jingrong Liu et al., 2019). Generally, the microbial spoilage of food will lead to changes in acidic and basic nature of food matrix or its surrounding environment due to the generation of organic acids, amines, ammonia and carbon dioxide (Alizadeh-Sani et al., 2021). Therefore, it is convenient to evaluate the food freshness by detecting the variation in pH values associated with the food, which can be visually indicated by pH–sensing dyes. Highlighted on the development of pH-sensing colorimetric film added with bioactive compounds, such as anthocyanins (Alizadeh-Sani et al., 2021; Luo et al., 2021; Roy, Kim, & Rhim, 2021; Shi, Zhang, Jia, Yang, & Zhou, 2021) to replace artificial pigments and dyes incorporated in the production of such packaging.

Anthocyanins are non-toxic potential natural food a type of flavonoids (phenolic phytochemicals), one of the plant's secondary metabolite (Roy et al., 2021), readily available, cost-effective, mainly represent the glossy orange, blue, purple, pink, and red colors of some plants' flowers and fruits (Roy et al., 2021), and may be extracted from different sources, such as plant products derivatives and food waste (Cheng et al., 2022; W. Yang et al., 2022). Furthermore, anthocyanins also have some other special functional effectiveness including antioxidant and antimicrobial activities, which may be favorable to the stabilization of foodstuffs and extension of their shelf life (Silva, Costa, Calhau, Morais, & Pintado, 2017). Among the various sources of anthocyanins, calyxes, or Roselle flowers, calyxes, or Roselle flowers (Hibiscus sabdariffa L.), also known as Hibiscus, were used in this study. Hibiscus aqueous extract (HAE) is an accessible source, with a high amount of anthocyanins (1.5 g/100 g on a dry weight basis) (Degenhardt, Knapp, &

* Corresponding author at: Juliana Farinassi Mendes, Nanotechnology National Laboratory for Agriculture (LNNA), Embrapa Instrumentação, Rua XV de Novembro, 1452, São Carlos, SP 13560-970, Brazil.
E-mail address: julianafarinassi@gmail.com (J.F. Mendes).

https://doi.org/10.1016/j.foodres.2022.111914
Received 15 April 2022; Received in revised form 18 July 2022; Accepted 7 September 2022
Available online 11 September 2022

Winterhalter, 2000). HAE contains pectin, ascorbic acid, and phenolic compounds that offer health benefits due to its various pharmacological and functional activities (antibacterial, anti-inflammatory, antihypertensive, antifertility, and antifungal) (Grajeda-Iglesias et al., 2016; Maciel et al., 2018). In addition, some studies have reported the HAE's color changes ability as a function of pH variation, with the same behavior when incorporated into polymeric films (Peralta, Bitencourt-Cervi, Maciel, Yoshida, & Carvalho, 2019). Zhai et al., (2017) when developing colorimetric films using Roselle anthocyanins, starch, and PVA, reported the gradual change from purple to green and then to a yellow coloration.

However, most of the current studies have shown direct incorporation of the anthocyanins extract into polymer matrices (Alizadeh-Sani et al., 2021; Giusti & Wrolstad, 2001; Grajeda-Iglesias et al., 2016; Jiang et al., 2020; Pereira, de Arruda, & Stefani, 2015; Shi et al., 2021; Singh, Nwabor, Syukri, & Voravuthikunchai, 2021; W. Yang et al., 2022; Zhai et al., 2017), which may affect its stabilization and bioavailability due to physical and chemical factors (e.g., environmental conditions and during its application). Given the sensitivity of this pigment, the microencapsulation of HAE as a possibility to maintain the stability of its antioxidant compounds when exposed to unfavorable conditions is a viable alternative and a promising technology to preserve its functionality (Nogueira, Fakhouri, Velasco, & de Oliveira, 2019). Encapsulation is defined as a technique in which substances in the solid, liquid, or gaseous state (encapsulated agent or active core) are packaged with an encapsulating agent (wall or shell material) (Tarone, Cazarin, & Marostica Junior, 2020). This is a technique that may solve this issue, as highlighted in other recent studies to protect the bioactive compounds from adverse environmental conditions (Sakulnarmrat & Konczak, 2022; Sharif, Khoshnoudi-Nia, & Jafari, 2020; Tarone et al., 2020). Sharif et al., (2020) reported that spray drying is the most popular technique among the ones studied for anthocyanins encapsulation. Initially, anthocyanins spray drying involves choosing to encapsulate agents, such as biopolymers maltodextrin (MD) and inulin (IN), which improve the encapsulation stability (da Silva Carvalho et al., 2016; Jimenez-Gonzalez et al., 2018; Mar et al., 2020). Akhavan Mahdavi, Jafari, Assadpoor, & Dehnad, (2016), when studying the complexation of anthocyanin-rich extract with maltodextrin and gum arabic by spray drying. They observed encapsulations with improved physical properties (moisture content, hygroscopic, agglomeration and solubility level), among other properties that microparticles must exhibit depending on their application.

Nowadays, pH–sensing indicators have received growing attention in food freshness monitoring due to their versatile fabrications and easily distinguishable visual color variations (Zhai et al., 2018). Some typical pH–sensing indicators have been successfully applied to monitor quality of shrimp (Kang et al., 2018; Jingrong Liu et al., 2018; Ma, Du, & Wang, 2017; Ma, Ren, Gu, & Wang, 2017), fish (Huang et al., 2019) (Ma, Du, et al., 2017; Ma, Ren, et al., 2017), pork (Choi, Lee, Lacroix, & Han, 2017; Zhang, Zou et al., 2019) and milk (Ma & Wang, 2016; Pereira et al., 2015).

Moreover, as reviewed in other studies, only a few researchers have focused on the correlation between structural, physical, and functional indication characteristics of anthocyanins encapsulated by spray drying with film-forming substrates (Luiza Koop et al., 2022; Santos, Rodrigues, Costa, & Madrona, 2019). As mentioned earlier, there is a lack of research on the incorporation of anthocyanins encapsulated by spray drying technique into biopolymer matrices.

In this context, this study aimed to analyze the influence of spray drying technique in HAE encapsulation combining different encapsulating agents (Maltodextrin - MD and Inulin -IN) on the production and physical and chemical properties of pectin-based biodegradable colorimetric films (varying the concentration of the incorporated HAE anthocyanins microparticles), as a way of mapping out different components and their interactions on microparticles and biopolymer matrix characteristics. To the best of our knowledge, this is the first study on attaining pectin intelligent pH indicator film by varying HAE concentrations that were produced continuously using a pilot-scale lamination unit. The continuous casting time is extremely shorter than those required for batch casting of most edible films. This denotes its main advantage. The shorter time required for drying may avoid phase separation in a heterogeneous mixture, improving therefore the properties of the film when compared to batch casting (Manrich et al., 2017). The films obtained by continuous casting were tested for their coloration change ability as a function of different pHs. We hypothesized that colorimetric biopolymer films obtained from pectin matrix (HM) incorporated into anthocyanins-HAE microparticles, with combination of wall materials and different concentrations, could increase the efficiency of the functional properties, as well as their barrier and mechanical properties., because both IN and MD wall materials, as well as their combinations, allow for better encapsulation efficiency (Araujo-Díaz, Leyva-Porras, Aguirre-Bañuelos, Álvarez-Salas, & Saavedra-Leos, 2017; Fernandes, Borges, & Botrel, 2014), as well as polysaccharides with structures similar to HM, serving as possible fillers and reinforcement (de Oliveira Filho et al., 2021), in addition to allowing the assessment of possible interactions with the matrix, since the anthocyanin molecules are associated differently with each polymer (Deng & Zhao, 2011). In the present work, HAE microparticles encapsulated with inulin (IN, concentration 1:1 and 1:4), maltodextrin (MD, 1:1 and 1:4) and their combinations (IN/MD, 1:1 and 1: 4) were incorporated with 10 and 20 % w/w HM. In addition, the biopolymeric colorimetric films were obtained by the continuous casting technique, and their potential use to obtain new food packaging was evaluated.

2. Materials and methods

2.1. Materials

High-methoxylation-degree pectin (HM) (DM > 50 %; Mw = 130,000 g.mol^{-1}) was supplied by CP Kelco (Limeira-SP, Brazil). The carrier agents used in the spray drying were inulin (IN) with a > 10 polymerization degree (OraftiGR, BENEO-Orafti, Tienen, Belgium) and maltodextrin (MD) (DE-12–20). Hibiscus (*Hibiscus sabdariffa*) was purchased from local retailers. Glycerol was obtained from Synth (Rio de Janeiro-RJ, Brazil). 2.2-diphenyl-1-picrylhydrazyl (DPPH) and 6-hydroxy-2,5,7,8-tetramethylchroman-2-carboxylic acid, or Trolox (Sigma-Aldrich Co. LLC, USA) were used as received.

2.2. Extraction of hibiscus e anthocyanins

Hibiscus calyxes extract (HAE) that was rich in anthocyanins was prepared according to the literature with a slight modification (Abdelghany, Menazea, & Ismail, 2019; Chumsri and Sirichote Anchalee, 2008). Approximately, 5 g hibiscus calyxes were added to 100 mL of distilled water and heated at 60 °C for approximately 60 min. Then, the extract was filtered and stored under refrigeration.

2.3. Microencapsulation of hibiscus anthocyanin-rich extract

HAE microparticle's were prepared using the spray drying technique according to Carmo et al., (2019) and A Figueiredo et al., (2020), with slight modifications. For the microparticle's production, feed solutions contain 100 g of HAE, MD and IN. The solutions were prepared by varying the carrier agents (IN and MD) and their ratios (1-1 and 1-4, in relation to HAE), as follows: Inulin (IN/ HAE, 1:1 and 1:4), Maltodextrin (MD/HAE, 1:1 and 1:4) and their combinations (IN/MD/HAE, 1:1:1 and 1:1:4). Table 1 described the proportions used for the microparticle's formulation. The solutions were prepared using a homogenizer (Ultra-Turrax IKA T18 basic, Wilmington, USA) under stirring at 5000 rpm for 30 min. Then, the solutions were dried by spray-drier (Model MSD 1.0; Labmaq do Brasil, Ribeirão Preto, Brazil) equipped with a two-fluid nozzle atomizer made of a tip with a 0.7 mm internal opening, at 8 ±

Table 1
Proportions of Hibiscus anthocyanin-rich extract (HAE), maltodextrin (MD) and inulin (IN) used for the microcapsule's formulation.

Sample	HAE(g)	Inulin (g)	Maltodextrin (g)
IN/HAE-1:1	50	50	
IN/HAE-1:4	75	25	
MD/HAE-1:1	50		50
MD/HAE-1:4	75		25
IN/MD/HAE-1:1:1	50	25	25
IN/MD/HAE-1:1:4	75	12.5	12.5

2 g. min^{-1} feeding rate, 35 L.min^{-1}drying airflow, with a 120 °C inlet temperature and approximately 85 °C outlet temperature. The resulting powders were collected from the cyclone and stored in a desiccator, away from light, at room temperature for further analysis and application to films.

2.4. Films-forming protocol

Control pectin films and pH-sensing colorimetric film incorporated with HAE microparticle's were prepared according to studies by Mendes, Norcino, Manrich, et al., (2020) and Mendes, Norcino, Martins, et al., (2020a), following the procedure shown in Fig. 1.

Indicator composite films were prepared by adding 10 and 20 % w/w of pre-prepared HAE microparticle's powders (IN/HAE-1:1, IN/HAE-1:4, MD/HAE-1:1, MD/HAE-1:4, IN/MD/HAE-1:1:1 and IN/MD/HAE-1:1:4). All films were homogenized, degassed, and molded into films in a KTF-S-B continuous lamination system (Mathis, Switzerland). The dried films were balanced out at 52 ± 3 % relative humidity (RH) and 25 ± 2 °C.

2.5. Characterization of calorimetric film

2.5.1. Infrared spectroscopy

Fourier-transform infrared spectroscopy (FTIR) were acquired by a Vertex 70 spectrophotometer (Bruker, Germany). Spectra were recorded from 4000 to 400 cm^{-1} at 32-scan rate and 4 cm^{-1} spectral resolution using an attenuated total reflectance (ATR) module.

2.5.2. X-ray diffraction (XRD)

The crystalline structures of the films were analyzed through diffraction patterns obtained on a XRD-6000 X-ray diffractometer (Shimadzu, Kyoto, Japan). Samples were scanned from 5 to 40 ° (2ɵ) at 1°. min^{-1}. Crystallinity index (CI) was determined based on the areas under the Gaussian-deconvoluted crystalline and amorphous peaks after baseline correction, according to the Eq. (1) (Alamri & Low, 2010):

$$C(\%) = \frac{Ac}{Ac + Aa} \times 100 \quad (1)$$

where Aa and Ac represents the area referring to the amorphous and crystalline part, respectively, of HM and HM / anthocyanin-HAE microparticles.

2.5.3. Scanning electron microscopy (SEM) observation

SEM observation micrographs of the samples were examined under a by Scanning Electron Microscopy (SEM) (JEOL JSM-6510) operating at 5 kV. All specimens were sputter-coated with gold (Balzer, SCD 050).

2.5.4. Mechanical properties

Films were submitted to uniaxial tensile assay on a DL3000 universal testing machine (EMIC, São Paulo-SP, Brazil). Tests were carried out according with ASTM D822-09 (ASTM D882-09, 2009) and other studies (Abral et al., 2019; Gouveia, Biernacki, Castro, Gonçalves, & Souza, 2019; Saricaoglu, Tural, Gul, & Turhan, 2018). At least six 15-mm wide, 100-mm long, and *ca.* 0.8-mm thick (measured using an IP65 Mitutoyo digital micrometer at five random positions) specimens per treatment were stretched at 25 mm min^{-1} using an initial clamp-to-clamp distance of 50 mm and a 50-kgf load cell. The elastic modulus (E) was determined from the linear slope of the stress versus strains curves. The tensile strength (σ_{max}) was calculated by dividing the maximum force by the initial cross-sectional area. Elongation at break (ε) was calculated by Eq. (2), wherein d is the final displacement and d_0 is the initial clamp-to-clamp distance:

$$\varepsilon(\%) = \frac{d - d_0}{d_0} \times 100 \quad (2)$$

Through the values obtained in the stress versus strain graphs, the

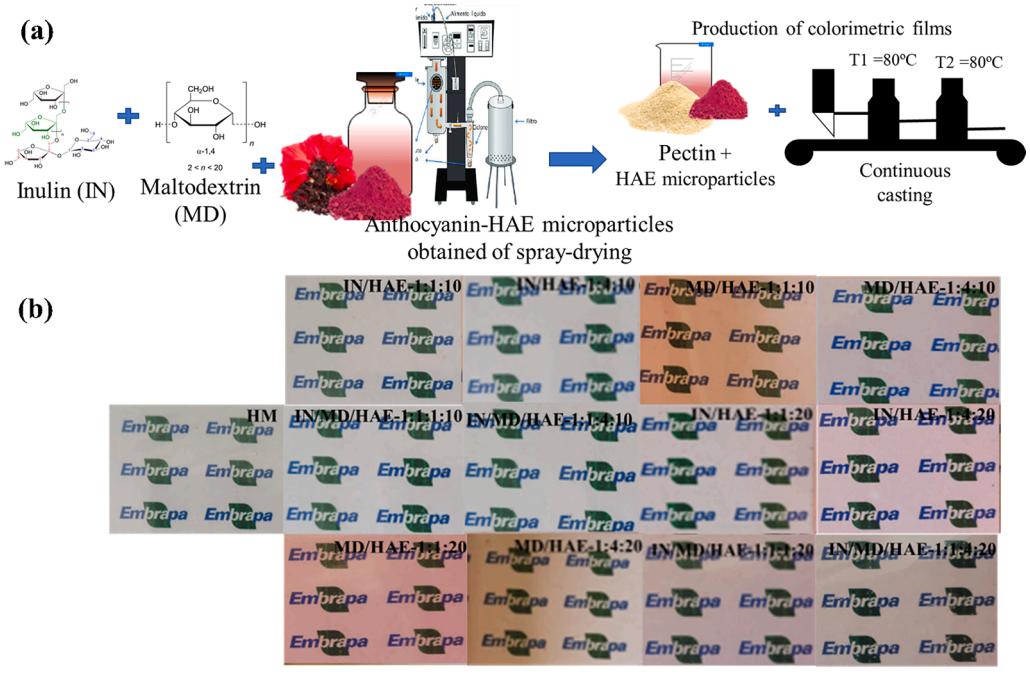

Fig. 1. (a) Representation of the method for obtaining colorimetric indicator films based on pectin (HM) and anthocyanin-HAE microparticles; (b) Images of colorimetric films obtained by continuous casting.

toughness of the films was calculated for the area below the curve.

2.5.5. Water vapor permeability (WVP) and moisture content (MC)

The water barrier properties of the films were determined using a modified ASTM method E96/16 (ASTM E96, 2016). The sample were cut into circles and sealed on the top of permeation cells containing dried silica gel to provide constant RH. The cells were then stored in a desiccator containing distilled water (100 % RH; 2.337 × 10^3 Pa vapor pressure at 20 °C). Afterwards, the amount of water vapor transferred through the film was quantified gravimetrically over 8 h. *WVP* (g.mm.kPa^{-1}.h^{-1}.m^{-2}) was calculated by Eq. (3):

$$WVP = \frac{W \times \delta}{A \cdot t \cdot \Delta P} \quad (3)$$

where *W* is change in cell weight [g], δ is average film thickness [m], and *A*, *t*, and ΔP are exposed film area [m^2], time [s], and partial water vapor pressure differential [Pa], respectively. The average WVP value for each sample was obtained in triplicates.

The moisture content (MC) of films was determined by thermally drying to an equipoise weight at 105 °C in an oven. MC was calculated based on the following Eq. (4).

$$MC(\%) = 100^{*}(\frac{Mi \times Mf}{Mi}) \quad (4)$$

where Mi was the initial weight of films stored in 75 % RH to moisture equilibrium (g) and Mf was the final weight of films dried at 105 °C (g).

2.5.6. Thermal properties

The thermal degradation profiles of the samples (*ca.* 6 mg) were obtained on a TGA Q500 (TA Instruments, USA), from 25 to 600 °C at 10 °C.min^{-1}, within a synthetic air atmosphere. Differential Scanning Calorimetry (DSC) analysis was performed using a differential scanning calorimeter (TA Instrument Q100). The measurements were made on the samples of 6.5–7 mg obtained from a central part of the injection molded standard dumbbell-shape specimens in the temperature range between 20 and 200 °C under nitrogen atmosphere (60 mL.min^{-1}). All measurements were taken according to the following program: heated between 20 and 200 °C at a scanning rate of 10 °C.min^{-1}, maintained at 200 °C for 1 min, and cooled between 200 and 20 °C at a scanning rate of 5 °C.min^{-1}. The whole process was carried out twice to analyze processing memory/history of the materials (the first heating–cooling cycle) and the thermal properties of the composites (the second heating–cooling cycle). An empty pan was used as a reference. Crystallization and melting parameters as: crystallization temperature (Tc), melting temperature (Tm), melting enthalpy (ΔHm), and crystallization enthalpy (ΔHc).

2.5.7. Optical properties

Film color and opacity were determined using a Konica Minolta CM-5 colorimeter (Minolta Camera Co., ltd, Osaka, Japan). A white standard color plate ($L = 97.76$, $a = -0.26$, $b = -0.44$) was used for calibration and as background before luminosity (L^*) as well as the chromatic coordinates a^* and b^* were determined by reflectance according to the CIE L^*, a^*, and b^* scale. The color parameters were used to calculate total color difference (ΔE^*, Eq. (5)).

$$\Delta E^{*} = \sqrt{(\Delta L^{*})^2 + (\Delta a^{*})^2 + (\Delta b^{*})^2} \quad (5)$$

2.5.8. Total monomeric anthocyanins (TMA), total phenolic compounds (TPC), and antioxidant capacity

Total monomeric anthocyanins (TMA), total phenolic compounds (TPC), and antioxidant capacity were obtained for HAE, microparticle's powders, and films. TMA content was determined using the pH differential method described by AOAC (2006), Giusti & Wrolstad (2001), and da Silveira et al. (2019). TPC was determined according to the Folin-Ciocalteu spectrophotometric method described by Singleton, Orthofer, & Lamuela-Raventós (1999). Antioxidant activity was determined as described by Brand-Williams, Cuvelier, & Berset, (1995) and Franco et al., (2020).

2.5.9. Color stability

The color stability of the colorimetric films were performed according to the studies of Jialin Liu, Huang, Ying, Hu, & Hu, (2021), Zhai et al., (2017) and Z. Yang et al., (2021). The pH sensing films was firstly cut into a disc in diameter of 2 cm and submerged in pH 3,4,7 and 10 buffers solutions for 10 min. Then, the film color was determined by using a portable colorimeter (Minolta Camera Co., ltd, Osaka, Japan). L* (lightness), a* (redness-greenness), b* (yellowness-blueness) were measured to evaluate the color of the films. Three measurements were taken on each film. The total color difference (ΔE) was calculated according to Eq. (5).

2.6. Statistical data treatment

The results were submitted to analysis of variance (ANOVA) and multiple comparison Tukey test, both at a 5 % significance level ($p < 0.05$), using the statistical software Sisvar® (Version 5.4).

3. Results and discussions

3.1. Infrared spectroscopy analysis

ATR-FTIR spectroscopy was carried out to find possible interactions among HM, HAE and wall materials (IN/MD) and the films' chemical structure. The spectra are shown in Fig. 2 and S1.

HM films showed characteristic bands around 3342, 2936, 2865, and 1009 cm^{-1}, attributed to the inter- and intramolecular –OH free stretching vibration (Nisar et al., 2018) –CH stretching (Nisar et al., 2018), and the structure's –COC stretching vibration, respectively (Azeredo et al., 2016). Typical HM bands were also found in the spectra of films incorporated with HAE encapsulated with either IN, MD (1:1 or 1:4) or their combinations (IN/MD/HAE, 1:1:1 or 1:1:4) at 10 and 20 % wt. % (in relation to HM mass) (Fig. 2a and b). This suggests that the addition of anthocyanins-HAE microparticles had no effect on HM's chemical structure, as characteristic bands resulting from the MD/IN powders and their combinations like those of HM were observed (Fig. S1), which overlap. This is in line with similar systems comprising different biopolymer matrices for encapsulation (Miranda-Linares, Quintanar-Guerrero, Del Real, & Zambrano-Zaragoza, 2020; Moghbeli, Jafari, Maghsoudlou, & Dehnad, 2019). Furthermore, this may suggest that the matrix successfully covered the encapsulated anthocyanins, as seen in Fig.S1; also observed by Mehran, Masoum, & Memarzadeh, (2020). However, when compared with the HM spectrum, the band's intensity at 1650 cm^{-1} in the film's spectrum added with anthocyanins-HAE microparticles (HM/IN/HAE, HM/MD/HAE, and HM/IN/MD/HAE) with 10 % (Fig. 2a) and 20 % (Fig. 2b) increased. This band corresponds to –CC aromatic ring elongation vibration (Jiang et al., 2020). According to Jiang et al., (2020) and Prietto et al., (2017) the apparent increase in this band intensity showed that anthocyanins-HAE microparticles were incorporated into the HM matrix. Furthermore, the intensity of the band assigned to hydroxyl stretching vibration (3700–3000 cm^{-1}) was narrower and higher after adding anthocyanins-HAE microparticles, possibly indicating the formation of new hydrogen bonds between anthocyanins and HM (Pourjavaher, Almasi, Meshkini, Pirsa, & Parandi, 2017). This narrowing in the 3700–3000 cm^{-1} bands possibly indicates the film's hydrophilicity decrease. It agrees with the WVP results, as to be discussed later in this study.

3.2. X-ray diffraction (XRD) analysis

XRD was used to analyze the crystal structure and evaluate the

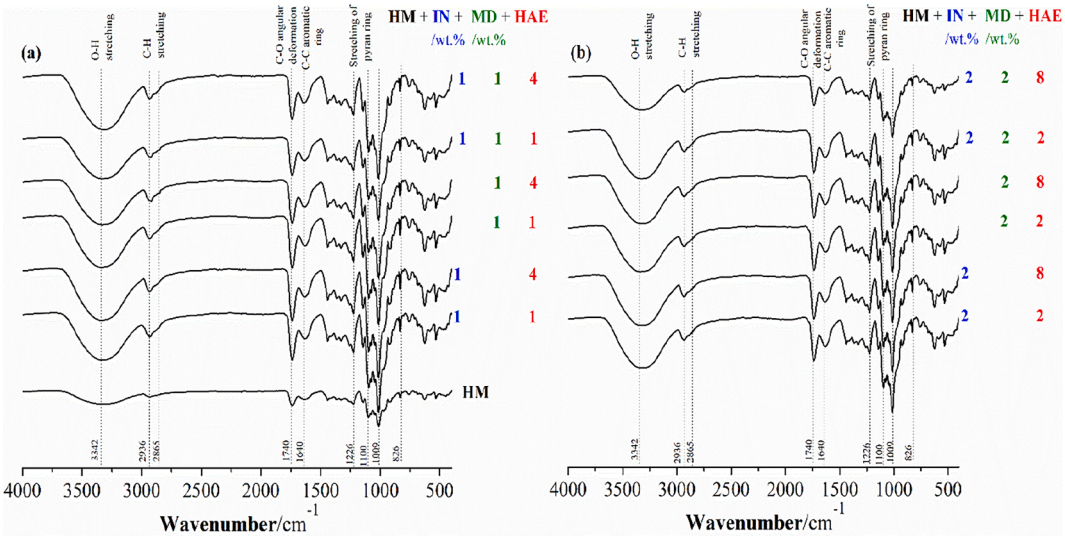

Fig. 2. Attenuated Total Reflectance-Fourier-Transform Infrared spectra of pectin films (HM) and various indicator films with 10% (a) and 20% (b) encapsulated anthocyanin content (Inulin/Maltodextrin/Hibiscus aqueous extract – IN/MD/HAE).

compatibility among HM, IN, MD, HAE and their combinations. Fig. 3 shows the XRD patterns for the encapsulated anthocyanins HM films and those containing IN, MD, IN/MD/HAE.

The XRD patterns were observed for the control film, i.e., only HM evidenced a semicrystalline pattern with peaks centered at 2ϴ = 13 and 20° (Almasi, Azizi, & Amjadi, 2020; Nisar et al., 2018). In the case of IN/HAE, MD/HAE, and IN/MD/HAE encapsulated anthocyanins-HAE microparticles, a broad peak was observed around 19.6°, which indicates its amorphous structure (Fig. 3a). Similar amorphous structures have also been reported for anthocyanins from black carrots and purple sweet potato (Fraga, Galleano, Verstraeten, & Oteiza, 2010; Koosha & Hamedi, 2019), as well as for the IN and MD wall materials (Zimeri, 2002). Anthocyanins-HAE microparticles loading caused an XRD pattern change of HM/IN/HAE (Fig. 3b), HM/MD/HAE (Fig. 3c), and HM/IN/MD/HAE (Fig. 3d) films, i.e., the position and intensity of all peaks related to HM's semicrystalline nature were affected by the incorporation of IN/HAE, MD/HAE and their combinations. Thus, it was found that anthocyanins-HAE microparticles with different wall materials (IN or MD), the ratio between IN/MD and HAE and the concentration added in the films (10 or 20 %) interfered with the intra- and intermolecular

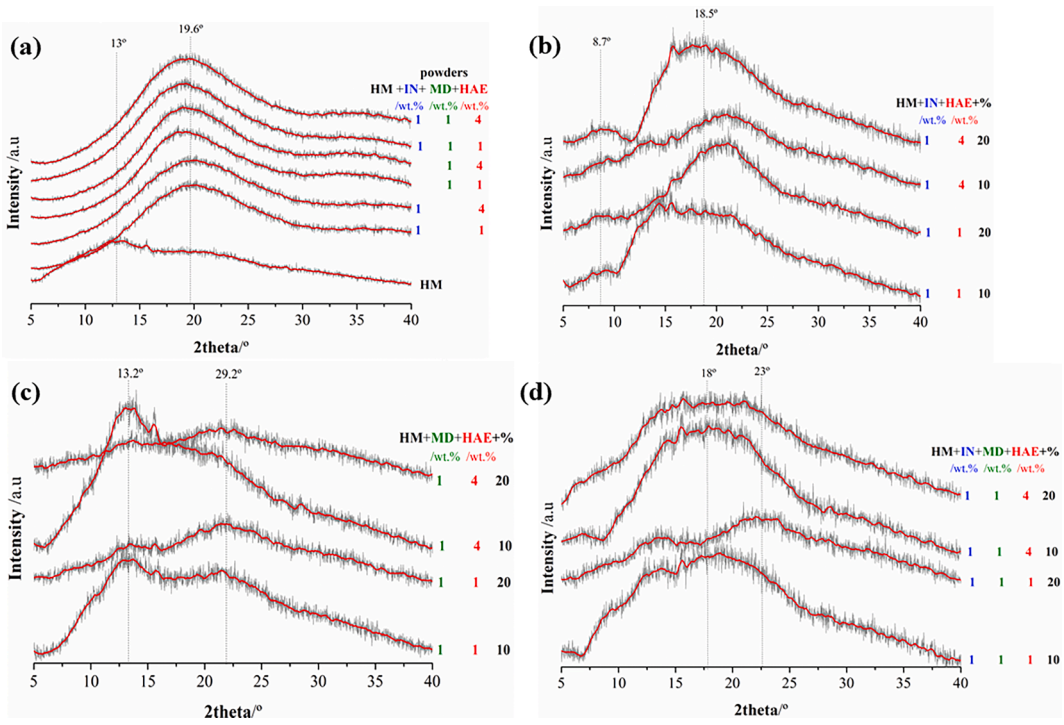

Fig. 3. X-ray diffraction patterns of pectin (HM)-based films and encapsulated anthocyanin powers (a); HM films added with anthocyanins encapsulated using different wall materials: inulin (IN) (b), maltodextrin (c) and inulin/maltodextrin (IN/MD) combination (d) at different ratios (1:1 and 1:4) and concentrations (10 and 20%) added in the films. Gray curve: actual data – used for calculations; red curve: smoothed – used for representation only. (For color references interpretation in this figure's caption, the reader is referred to the Web version of this manuscript). (For interpretation of the references to color in this figure legend, the reader is referred to the web version of this article.)

hydrogen bond formation in HM itself, which agrees with the FTIR spectra (Fig. 2). Furthermore, it was observed that increasing the concentration of anthocyanins-HAE microparticles added into HM films (i.e., 20 % w/w HAE encapsulated compared to HM) decreased the diffraction intensity. However, this was not seen with increasing HAE incorporation into the microparticles (1:4 ratio). According to Zabot, Silva, Azevedo, & Meireles, (2016), these changes in the structures may be associated with a physical interaction among the wall materials' molecules (IN and MD), HAE, and HM, suggesting that the encapsulated bioactive compounds are present in the polymer matrix. This agrees with the crystallinity index of the film samples, as presented in Table 1. The crystallinity indexes (Table 2) of the control film sample were 17 % (HM), 12–19 % (IN/HAE-1:1 and 1:4), 16–28 % (MD/HAE-1:1 and 1:4) and 14–29 % (IN/MD/HAE-1:1 and 1:4). The increased crystallinity in the films by IN/MD combination may influence active compounds release, as higher activation energy is required to dissolve the crystals when compared to the amorphous film (L. Wu, Zhang, & Watanabe, 2011). Yu, (2001) e Zabot et al., (2016) stated that films with higher crystallinity are less hygroscopic and soluble than amorphous materials, which may be observed in the current study (Table 3).

3.3. Scanning electron microscopy (SEM)

Scanning electron microscopy (SEM) images for pectin (HM) films, as well as HM/IN/HAE and HM/MD/HAE and HM/IN/MD/HAE composite films' surface and cross-section images are shown in Fig. 4a and 4b, respectively. Fig. S2 shows the microparticles external microstructure with irregular surfaces, spherical shapes, and different sizes, features usually found in samples obtained by spray drying.

The HM-only film surface was homogeneous, smooth, and uniform (Fig. 4a). Overall, regardless of the wall material (IN and MD) and concentration (1:1 and 1:4) used to encapsulate HAE, the HM/IN/HAE, HM/MD/HAE, and HM/IN/MD/HAE films showed slightly rough and uneven surfaces but presented a compact structure (fracture image) showing a good IN/HAE, MD/HAE distribution and their combinations in the HM matrix with low aggregation. For this, some studies have reported that the increased compactness might be due to strong interactions formation among IN, MD, HAE, and the film matrix (Mandal & Chakrabarty, 2019; Oun & Rhim, 2016; Zabihollahi, Alizadeh, Almasi, Hanifian, & Hamishekar, 2020), as shown by FTIR (Fig. 2) and XRD (Fig. 3) structural conformations. The strong interactions and compatibility among IN, MD, and HM may be related to the similar polysaccharide structure of these components.

Moreover, in the composite films fracture's SEM images (Fig. 4b), the films added with microparticles with higher HAE concentrations (1:4) showed smoother and more uniform surfaces especially those produced from MD and its combinations (IN/MD). This was verified with the 20 % w/w encapsulated anthocyanins microparticles incorporation (Fig. S2).

Table 2
Tensile attributes – tensile strength (TS), elongation at break (ε), elastic modulus (EM) and toughness (T) - as well as crystallinity index (IC %) – of pectin (HM)-based films and encapsulated anthocyanin powders with different wall materials of inulin (IN), maltodextrin and inulin/maltodextrin (IN/MD) combination, at different ratios (1: 1 and 1: 4) and concentrations (10 and 20%) added in the films.

Samples	Thickness/ μm	TS/ MPa	ε/%	EM/MPa	T/J. mm^{-3}	CI/ %
HM	32 ± 2^{a}	35.4 ± 3.2^{abc}	3.1 ± 0.1^{abc}	2151.4 ± 331.9^{a}	20.0 ± 3.2^{ef}	17
IN/HAE-1:1:10	35 ± 3^{a}	31.2 ± 5.0^{abc}	3.0 ± 0.6^{ab}	2321.9 ± 182.7^{a}	31.7 ± 5.2^{abc}	12
IN/HAE-1:1:20	35 ± 3^{a}	27.8 ± 8.1^{abc}	2.3 ± 0.5^{abc}	2289.0 ± 278.0^{a}	16.7 ± 5.5^{f}	19
IN/HAE-1:4:10	35 ± 3^{a}	35.0 ± 9.7^{ab}	2.5 ± 0.3^{abc}	2397.0 ± 409.3^{a}	35.4 ± 5.8^{ab}	14
IN/HAE-1:4:20	35 ± 3^{a}	25.4 ± 7.5^{bc}	2.1 ± 0.3^{bc}	2665.8 ± 423.3^{a}	22.2 ± 3.0^{def}	19
MD/HAE-1:1:10	35 ± 6^{a}	30.2 ± 8.8^{abc}	2.3 ± 0.7^{abc}	2341.6 ± 424.1^{a}	25.2 ± 7.3^{bcde}	16
MD/HAE-1:1:20	35 ± 3^{a}	39.5 ± 7.9^{a}	2.4 ± 0.5^{abc}	2771.8 ± 205.7^{a}	39.2 ± 6.0^{a}	28
MD/HAE-1:4:10	35 ± 5^{a}	23.1 ± 4.1^{bc}	2.0 ± 0.3^{c}	2680.6 ± 557.7^{a}	23.9 ± 3.8^{cdef}	19
MD/HAE-1:4:20	35 ± 2^{a}	28.5 ± 8.5^{abc}	1.9 ± 0.9^{bc}	2769.0 ± 237.3^{a}	34.8 ± 4.3^{ab}	14
IN/MD/HAE-1:1:10	35 ± 2^{a}	21.5 ± 5.4^{c}	1.7 ± 0.4^{c}	2103 ± 349.5^{a}	17.3 ± 4.2^{f}	14
IN/MD/HAE-1:1:20	35 ± 3^{a}	35.4 ± 9.3^{ab}	2.9 ± 0.7^{ab}	2193.0 ± 821.0^{a}	30.5 ± 2.6^{abcd}	20
IN/MD/HAE-1:4:10	35 ± 2^{a}	31.2 ± 9.2^{bc}	2.4 ± 0.5^{abc}	2095.1 ± 204.8^{a}	26.9 ± 5.4^{bcde}	29
IN/MD/HAE-1:4:20	35 ± 4^{a}	24.2 ± 4.2^{abc}	2.4 ± 0.6^{abc}	2717.1 ± 674.0^{a}	32.7 ± 5.0^{abc}	25

Mechanical attributes are reported as average values and standard deviations. Using Tukey's test, the same letters on the same column indicate the values were not statistically significant ($p > 0.05$).

Table 3
Water vapor transmission rate (WVTR), Water vapor permeability (WVP), Moisture content (MC), and thermal parameters – initial (Tonset) and final (Toffset) degradation temperatures – of pectin (HM)-based films and encapsulated anthocyanin powders with different wall materials of inulin (IN); maltodextrin (MD) and the inulin/maltodextrin (IN/MD) combination, at different ratios (1: 1 and 1: 4) and concentrations (10 and 20%) added in the films.

Samples	WVTR/g. m^{-2}.day^{-1}	WVT/g.mm. kPa^{-1}.day^{-1}. m^{-2}	MC/%	Tonset/ °C	Toffset/ °C
HM	44 ± 4^{a}	0.63 ± 0.08^{a}	7.1 ± 0.9^{b}	221	460
IN/HAE-1:1:10	39 ± 3^{abc}	0.63 ± 0.05^{a}	6.7 ± 0.9^{bc}	213	477
IN/HAE-1:1:20	42 ± 1^{abc}	0.63 ± 0.01^{a}	6.5 ± 0.7^{bcd}	217	474
IN/HAE-1:4:10	37 ± 3^{abc}	0.66 ± 0.01^{a}	7.4 ± 0.9^{b}	218	472
IN/HAE-1:4:20	39 ± 3^{abc}	0.56 ± 0.05^{a}	5.4 ± 1.4^{bcde}	217	468
MD/HAE-1:1:10	40 ± 3^{abc}	0.47 ± 0.01^{a}	11.2 ± 1.1^{a}	224	465
MD/HAE-1:1:20	37 ± 1^{abc}	0.57 ± 0.09^{a}	5.6 ± 0.9^{bcde}	225	472
MD/HAE-1:4:10	39 ± 3^{abc}	0.58 ± 0.09^{a}	3.1 ± 0.5^{e}	223	469
MD/HAE-1:4:20	40 ± 5^{abc}	0.60 ± 0.04^{a}	4.6 ± 2.0^{bcde}	221	465
IN/MD/HAE-1:1:10	43 ± 0^{ab}	0.49 ± 0.01^{a}	5.4 ± 1.7^{bcde}	222	472
IN/MD/HAE-1:1:20	33 ± 2^{c}	0.49 ± 0.07^{a}	3.7 ± 0.9^{de}	221	471
IN/MD/HAE-1:4:10	43 ± 2^{ab}	0.58 ± 0.05^{a}	5.1 ± 0.6^{bcde}	213	480
IN/MD/HAE-1:4:20	35 ± 3^{bc}	0.50 ± 0.08^{a}	4.1 ± 0.2^{cde}	227	476

Water vapor transmission rate (WVTR), Water vapor permeability (WVP), Moisture content (MC) were reported as average values and standard deviations. Using Tukey's test, the same letters on the same column indicate that the values were not statistically significant ($p > 0.05$).

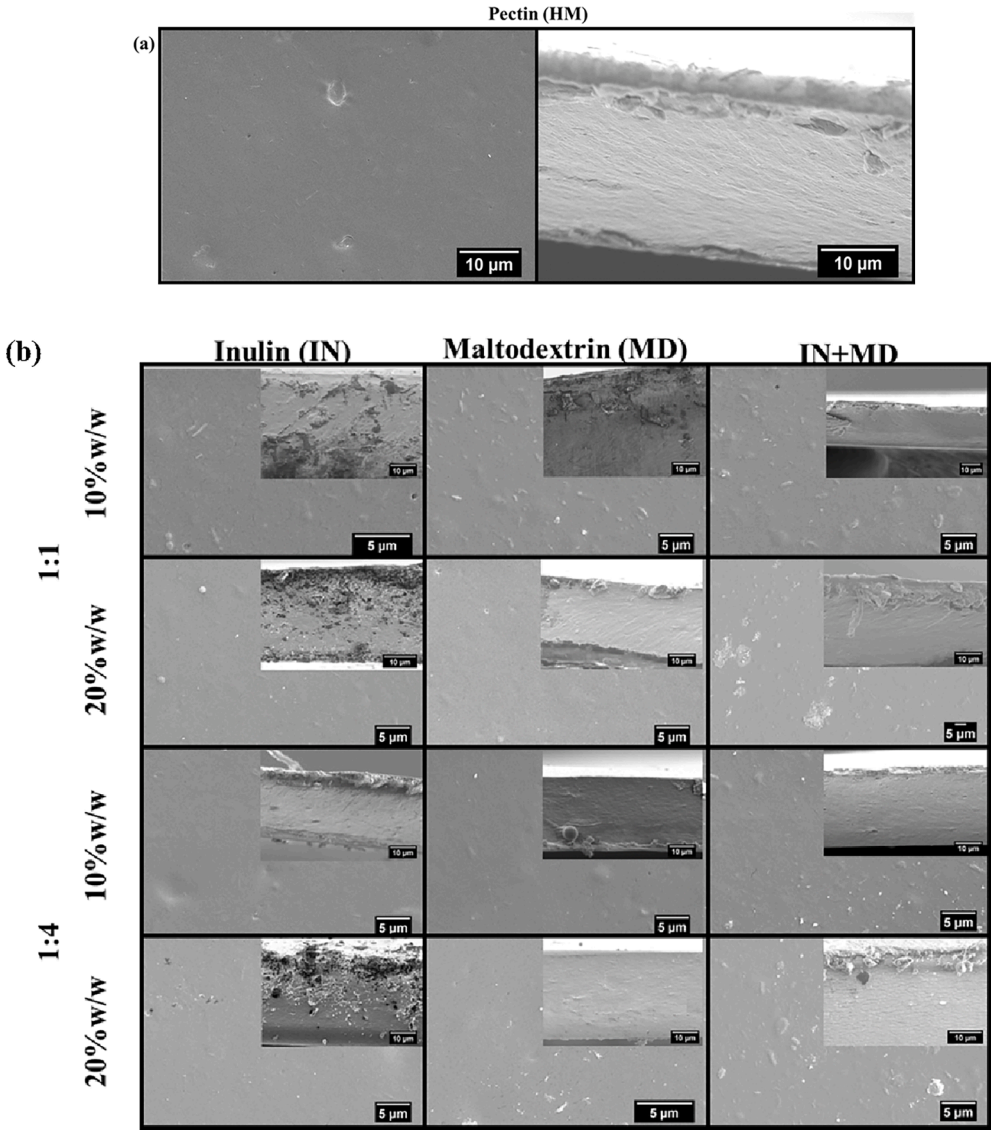

Fig. 4. Surface scanning electron microscopy (SEM) and cryogenic fracture images of pure pectin (HM) films (Fig. 4a) and pectin composites incorporated from encapsulated anthocyanin microparticles (Fig. 4b).

Nayak & Rastogi, (2010) observed smooth surfaces when MD with higher dextrose equivalents, such as DE 10–20, were used for anthocyanins encapsulation from *Garcinia indica* extract. According to Gharsallaoui, Saurel, Chambin, & Voilley, (2012), the occurrence of lower roughness in particles composed of higher DE polysaccharides may be attributed to their low viscosity when dispersed. The low molecular weight sugar presence may act as a plasticizer, preventing irregular microparticle surface shrinkage during the drying process. Therefore, MD with a high level of hydrolysis, as used in this study, produces a higher amount of smooth particles, as observed in Fig. S2. Da Silva Carvalho et al., (2016), observed that smoother particles present higher anthocyanins retention, which may be linked to better pigment accommodation in the particle. However, IN/MD/HAE-1:1:20 and IN/MD/HAE-1:4:20 films showed cracks on their fracture surfaces, which could form agglomerates and disrupt the HM network compaction. As a result, films homogeneity was reduced, and they showed a rough cross-section (Koshy et al., 2021; Zhai et al., 2017). Thus, the encapsulated HAE microparticle's surfaces and distributions interfered with the film's morphologies, as evidenced in Fig. 4b and S2 and Table S1.

3.4. Mechanical test

The mechanical properties - tensile strength (TS), elongation at break (ε), elastic modulus (EM) and toughness (T) - of HM control films and the composites added with different IN/HAE, MD/HAE, and IN/MD/HAE microparticles concentrations were investigated. The results are presented in Table 2 and Fig. S3.

HM pure film thickness was 35 µm, maintained for the other films HM/IN/HAE, HM/MD/HAE, HM/IN/MD/HAE (Table 2), even after encapsulated HAE incorporation. This shows the efficiency in standardizing the film's attainment by continuous casting technique. A similar phenomenon was reported in other studies by the group (Mendes et al., 2019a, 2019b, Mendes, Norcino, Manrich, et al., 2020).

Overall, a reduction in TS (35.4–23.1 MPa) and ε% (3.1–1.7 %) (Table 2) by approximately 35 % and 45 %, respectively, occurred, although no statistical difference was observed among films. This may be attributed to possible defect points and stress concentration in the films after encapsulated HAE microparticles incorporation (Etxabide, Maté, & Kilmartin, 2021), except for samples IN/HAE-1:4:10 (35 MPa and 2.5 %) and MD-1–1-20 (39.5 MPa and 2.4 %). The HM composite films showed distinct mechanical behavior for the types and

concentrations of the wall materials used for the encapsulated HAE microparticles production, as seen in Table 2. Azeredo et al., (2016) found a tensile strength of 7.4–4.4 MPa for a smart pectin composite with citric acid-containing pomegranate juice anthocyanins. Thus, the tensile strength values reported in our study were higher than the ones from studies based on polysaccharides and anthocyanins (Eça, Machado, Hubinger, & Menegalli, 2015; Pereira et al., 2015). Furthermore, a significant increase in EM was observed in the films ($p < 0.05$), making them stiffer as a function of increasing HAE microparticles concentration. These results may be due to reduced molecular chains mobility, as well as lower adsorbed water content (Table 3) - known for plasticizing biopolymer-based films (Mendes, Norcino, Martins, et al., 2020b).

When comparing the results of the IN/HAE, MD/HAE, and IN/MD/HAE composites with the polyethylene and polyethylene terephthalate (PET) mechanical properties, the composite films showed much lower specific stress than that of PET - about 38 % lower - and 52 and 37 % higher compared to low-density polyethylene (LDPE) and high-density polyethylene (HDPE), respectively. The indicator films' elastic modulus (2103–2772 MPa) was considerably higher when compared to PET (2100–3100 MPa), LDPE (200–400 MPa), HDPE (600–1400 MPa), PLA (350–2800 MPa), PA (1400 MPa), and PVC (25–1600 MPa).

3.5. Barrier property

The water barrier properties of HM-based films added or not by IN/HAE, MD/HAE, and IN/MD/HAE microparticles were analyzed using water vapor permeability (WVP) and water vapor transmission rate (WVTR) measurements, of which results are shown in Table 3. The WVTR is the rate of water vapour permeating through the film. In This work, the WVTR, is determined from the slope of the regression line of sample weight versus time graph whereby the slope is then divided by the area of the films being exposed to the transmission (Item 2.5.5), and WVP values calculated from the WVTR values (Eq. (3)).

The highest WVP (0.63 $g.mm.kPa^{-1}.day^{-1}.m^{-2}$) and WVTR (44 $g.m^{-2}.day^{-1}$) shown by the (HM) are found by the control films (HM), this is caused by hydrophilic hydroxyl groups gifts in pectin and glycerol (Maftoonazad, Neda Ramaswamy & Marcotte, 2007). Although the WVP of HM films and HM composites with HAE microparticle's with different wall materials (IN, MD, and IN/MD) and concentrations (10 and 20 % w/w) showed no significant difference ($p > 0.05$) (Table 3), the composites containing anthocyanins-HAE microparticles showed a *ca.* reduction by 11 % (HM/IN/HAE), 25 % (HM/MD/HAE), and 22 % (HM/IN/MD/HAE), respectively. This was also seen for the WVTR values (HM/IN/HAE and HM/MD/HAE − 14 % and HM/IN/MD/HAE − 19 %). Furthermore, the increase in barrier properties was more pronounced in the composite films incorporated at 10 % w/w added with anthocyanins-HAE microparticles obtained from single encapsulating materials, such as HM/IN/HAE and HM/MD/HAE films and in the films at 20 % w/w with microparticles obtained by encapsulating materials combination (MD/IN). Therefore, the type of wall material used and the microparticles concentration incorporated in the films affected the barrier properties. This may be related to the amount of polar groups (e.g., hydroxyl) in the molecular assembly (Milda E. Embuscado, 2009) and the increased crystallinity of films, as shown in Table 2. The incorporation of IN/HAE, MD/HAE, and IN/MD/HAE microparticles formed more crystalline HM-based films, consequently reducing pectin chains' mobility and rearrangement decreasing the availability of hydroxyl groups responsible for polysaccharide-water interactions, which resulted from hydrogen bonds formation between IN/HAE, MD/HAE and HM hydroxyl groups, as shown in the FTIR results (Fig. 2), corroborating with the studies by Alizadeh-Sani et al., 2021; Zhang, Liu et al., (2019). A uniform and interconnected matrix (Fig. 4), forming, which reduced water vapor diffusivity at the film interface may have contributed to such increase.

As for the influence of encapsulating materials (IN, MD and their combinations), in the WVP and WVTR values, Pereira Souza, Deyse Gurak, & Damasceno Ferreira Marczak, (2017), attributed to the dissociated electrostatic interactions between carboxylic pectin groups and the flavyl cation of anthocyanins. They also found that combining maltodextrin and pectin and increasing the added concentration allowed for a hydrophobic effect. A similar effect was reported by Sganzerla et al., (2021) for carboxymethyl cellulose (CMC)–based films and incorporated of different amounts of anthocyanin-rich blackberry extract (*Morus nigra L.*). Considering the WVP levels, the films produced here are suitable for use as moisture barriers in food packaging (Bedane, Eić, Farmahini-Farahani, & Xiao, 2015; Jiménez, Fabra, Talens, & Chiralt, 2010).

The MC (Table 3) of HM films (7.1 %) and of HM/IN/HAE (6.7–5.4 %), HM/MD/HAE (11.2–4.6 %) and HM/IN/MD/HAE (5.4–3.7 %) composites was significantly reduced ($p < 0.05$). According to Sganzerla et al., (2021), this may be due to the higher concentration of extract used in the formulation, which decreases absorption, and consequently swelling by water with the presence of anthocyanins. This corroborates with the WVP data since the extract incorporation changed the interaction between the films' component, decreasing the MC value (Zhai et al., 2017).

3.6. Thermal properties

The film's thermal property reflects its ability to resist decomposition at high temperatures. The thermogravimetric (TG) curves and their first derivatives (DTG) for HM-based films and their composites (HM/IN/HAE, HM/MD/HAE, and HM/IN/MD/HAE) are shown in Fig. 5(a-c). The corresponding temperatures for thermal degradation's initial (Tonset) and final (Toffset) are shown in Table 3.

HM-based films' thermal decomposition occurred in three distinct mass-loss stages; similar to the other composite films. The first one occurred at the 25–150 °C temperature range due to physical desorption of water and/or other volatile. The second one (*ca.* 180–230 °C) was attributed to sample's degradation, polymer and wall material constituents' depolymerization (Fernandes et al., 2017; Guo et al., 2021; Mendes et al., 2019a), and glycerol evaporation (boiling point = 182 °C). The third stage (around 450 °C, DTG peak) referred to pectin components degradation, forming carbonaceous materials (Mendes et al., 2019a). HM/IN/HAE and HM/IN/MD/HAE composite films showed a mass loss event at about 168 and 170 °C (DTG peaks), respectively, related to IN depolymerization (Zabot et al., 2016).

For the composite films, the HM-rich phase began to decompose at a slightly higher temperature (Table 3). The HM was thermally stable up to 221 °C, while the composite films were thermally stable up to 227 °C. The increased initial degradation temperature (Tonset) for composite films suggested that adding anthocyanins-HAE microparticles may have increased the molecular interactions between adjacent HM chains, and strengthened the hydrogen bonding between pectin, inulin, and maltodextrin's hydroxyl groups with the polar compounds (polyphenols) found in the anthocyanins (HAE), as shown by FTIR (Fig. 2) and XRD (Fig. 3). Composites HM/IN/HAE (1:1:10–20 % and 1:4:10–20 %) (45–57 %) HM/MD/HAE (1:1:10–20 % and 1:4:10–20 %) (51–57 %), and HM/IN/MD/HAE (1:1:1:10–20 % and 1:1:4:10–20 %) (45–55 %) showed lower mass loss at lower temperatures compared to HM (58 % mass loss), indicating that anthocyanin-HAE microparticles incorporation slightly increased the color indicator films' thermal stability. A similar result was found by Silva-Pereira, Teixeira, Pereira-Júnior, & Stefani, (2015), when adding red cabbage extract to chitosan/corn starch film. The films obtained in the current study showed stability at temperature below 100 °C, an essential requirement for food packaging.

Differential scanning calorimetry (DSC, Fig. 6) was analysed to assess the effect of IN/HAE, MD/HAE, and IN/MD/HAE microparticles incorporation on HM films' thermal stability. The melting temperature (Tm) of HM/IN/HAE (1:1:10–20 % and 1:4:10–20 %) (116–131 °C), HM/MD/HAE (1:1:10–20 % and 1:4:10–20 %) (125–135 °C), and HM/IN/MD/HAE (1:1:1:10–20 % and 1:1:4:10–20 %) (127–139 °C) films was

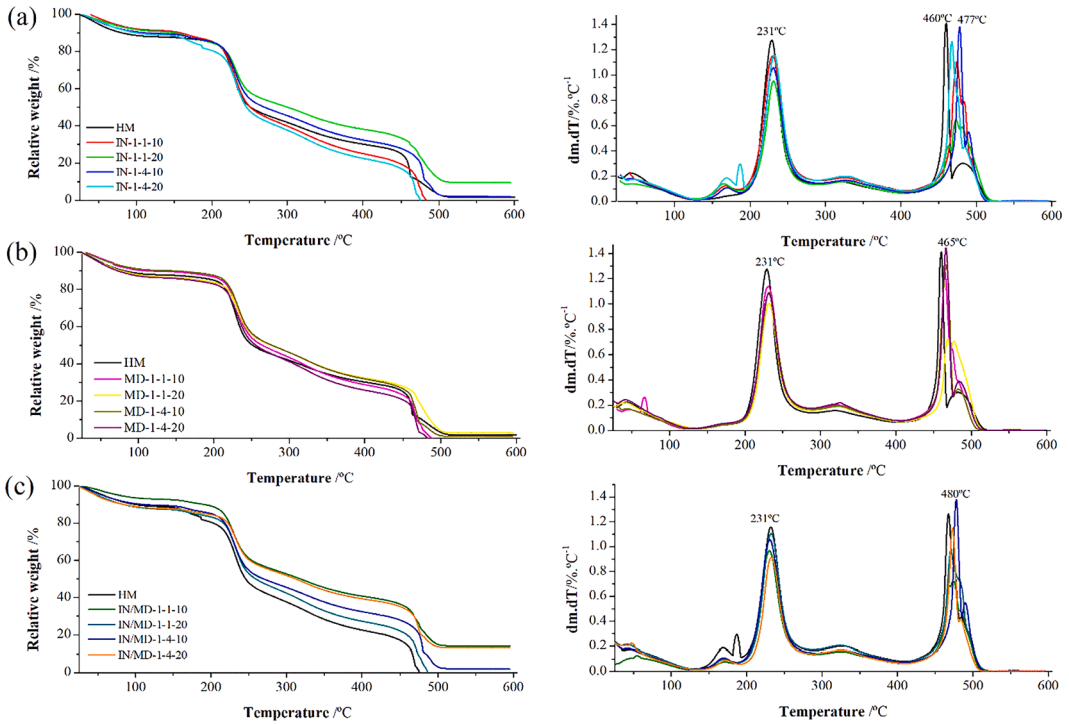

Fig. 5. Thermogravimetric (TG; left) and derivative (DTG, right) profiles of pectin (HM) films and of pectin (HM)-based films, and encapsulated anthocyanin powders with different wall materials of inulin (IN, a); maltodextrin (b) and the combination of inulin/maltodextrin (IN / MD, c), at different ratios (1: 1 and 1: 4) and concentrations (10 and 20%) added in the films.

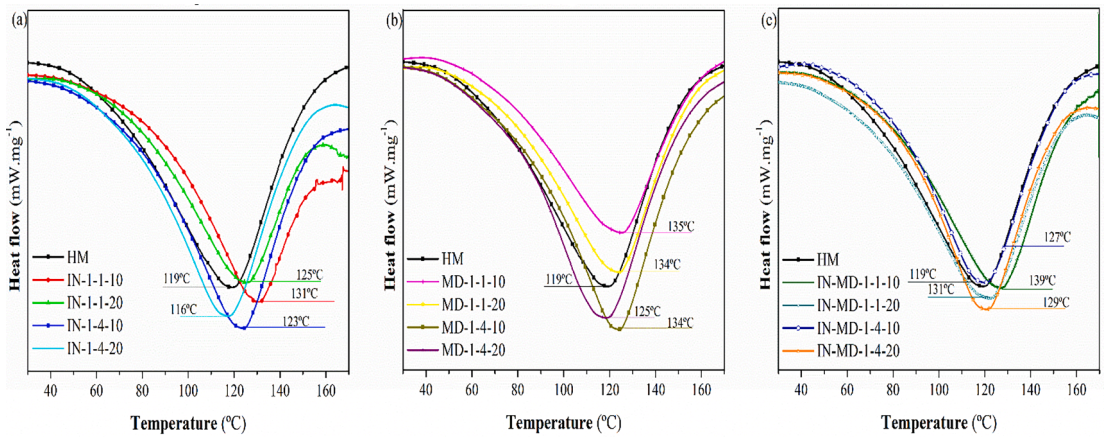

Fig. 6. Profile for pectin (HM) films and of pectin (HM)-based films and encapsulated anthocyanin powders with different wall materials: inulin (IN, a); maltodextrin (b), and inulin/maltodextrin combination (IN / MD, c), at different ratios (1: 1 and 1: 4) and concentrations (10 and 20%) added in the films.

significantly higher than that of the control film (HM, 119 °C). This showed that incorporating the anthocyanin microparticles encapsulated with IN and MD increased the pectin-based films' thermal stability, as seen in the thermogravimetric results.

3.7. Optical properties

The food packaging materials' color and transparency play an essential role in their appearance and customer acceptance. The effect of HAE microparticles on HM films colorimetric parameters is presented in Table 4.

The presence of anthocyanins-HAE microparticles in the films decreased L^* values (reduced lightness) (Table 4). The red-green (a^*) and blue-yellow (b^*) parameters increased significantly ($p < 0.05$) with increasing the anthocyanins-HAE microparticles (20 % w/w) compared to the control film. The effects were more significant when the films were developed at the 1:1 (wall material concentration - HAE) ratio and incorporated microparticles obtained from the individual wall materials (added only IN/HAE and MD/HAE). Thus, the HAE microparticles decreased the luminosity (L^*), while increasing the redness (a^*-*value*) and yellowing (b^*-*value*) in the films due to the red and yellow colors of anthocyanin and pectin, respectively (Rawdkuen, Faseha, Benjakul, & Kaewprachu, 2020; Roy et al., 2021). The total color difference (ΔE^*) values were calculated considering the HM film as standard. Despite reduction in L^* values reduction, all films showed high luminosity (i.e., L^* values close to 100), which is recurrent for edible films (Araujo-Farro, Podadera, Sobral, & Menegalli, 2010; Basiak, Lenart, & Debeaufort, 2017; Galus, 2018). As a result, the total color difference (ΔE^*) increased significantly ($p < 0.05$) by adding HAE microparticles to the films. According to Pająk, Przetaczek-Rożnowska, & Juszczak, (2019), films with

Table 4
Luminosity (L^*), chromatic coordinates (a^* and b^*), and colorimetric parameters (ΔE, total color difference) for pectin (HM) films and pectin (HM)-based films and encapsulated anthocyanin powders with different wall materials: inulin (IN); maltodextrin and the inulin/maltodextrin (IN/MD) combination, at different ratios (1: 1 and 1: 4) and concentrations (10 and 20%) added in the films.

Samples	L^*	a^*	b^*	ΔE	Apparent opacity /%
HM	87.0 ± 0.1^{a}	−1.0 ± 0.0^{j}	5.01 ± 0.06^{a}	6.2 ± 0.1^{j}	47.0 ± 9.0^{a}
IN/HAE-1:1:10	77.4 ± 0.3^{f}	12.6 ± 0.4^{e}	0.20 ± 0.01 ^{g}	20.0 ± 0.5^{e}	39.5 ± 1.8^{ab}
IN/HAE-1:1:20	67.0 ± 0.7^{j}	27.3 ± 0.9^{a}	3.06 ± 0.03^{L}	37.6 ± 1.1^{a}	44.2 ± 0.1^{ab}
IN/HAE-1:4:10	81.0 ± 0.1^{c}	7.3 ± 0.1 ^{h}	2.00 ± 0.07^{c}	13.5 ± 0.2 ^{h}	36.2 ± 6.0^{ab}
IN/HAE-1:4:20	76.1 ± 0.5 ^{g}	14.2 ± 0.3^{d}	−0.20 ± 0.16 ^{h}	21.6 ± 0.6^{d}	34.4 ± 2.0^{ab}
MD/HAE-1:1:10	76.0 ± 0.2 ^{g}	14.6 ± 0.3^{d}	−0.40 ± 0.01^{i}	22.1 ± 0.4^{d}	33.1 ± 0.6^{ab}
MD/HAE-1:1:20	66.2 ± 0.2^{j}	28.4 ± 0.4^{a}	−3.63 ± 0.03^{m}	39.0 ± 0.4^{a}	36.3 ± 3.2^{ab}
MD/HAE-1:4:10	78.5 ± 0.2^{e}	11.0 ± 0.2^{f}	0.67 ± 0.05^{f}	17.7 ± 0.3^{f}	41.0 ± 1.2^{ab}
MD/HAE-1:4:20	70.9 ± 0.2^{i}	22.0 ± 0.2^{b}	−2.20 ± 0.06 ^{k}	31.0 ± 0.3^{b}	39.4 ± 1.5^{ab}
IN/MD/HAE-1:1:10	79.8 ± 0.4^{d}	8.9 ± 0.4 ^{g}	1.52 ± 0.07^{d}	15.4 ± 0.6 ^{g}	36.2 ± 4.8^{ab}
IN/MD/HAE-1:1:20	72.6 ± 0.1 ^{h}	19.4 ± 0.4^{c}	−1.60 ± 0.04^{j}	27.9 ± 0.2^{c}	34.0 ± 1.5^{ab}
IN/MD/HAE-1:4:10	83.4 ± 0.1^{b}	3.0 ± 0.1^{i}	3.56 ± 0.07^{b}	9.1 ± 0.1^{i}	37.0 ± 1.2^{ab}
IN/MD/HAE-1:4:20	80.2 ± 0.2 ^{cd}	8.5 ± 0.2 ^{g}	1.38 ± 0.05^{e}	15.0 ± 0.3^{gh}	29.4 ± 1.3^{b}

Luminosity (L*), chromatic coordinates (a* and b*), and colorimetric parameters (ΔE, total color difference) are reported as average values and standard deviations. The same letters on the same column indicated that the values are not statistically significant ($p > 0.05$), using Tukey's test.

$\Delta E^* > 2$ show a difference in appearance compared to the control.

Light protection also plays a critical role in food packaging, as light may lead to vitamin degradation, fresh food's discoloration, development of off-flavors, and self-oxidation of fats (Duncan & Chang, 2012; Etxabide, Maté, et al., 2021). The control HM films showed higher transparency and higher light transmittance in the visible area. In contrast, HM/IN/HAE, HM/MD/HAE, and HM/IN/MD/HAE composite films presented strong UV light screening properties, significantly ($p < 0.05$) reducing light transmittance compared to control (HM) films (Table 4). Such characteristic is linked to anthocyanins ability to strongly absorb ultraviolet light due to their unique functional groups (C. Wu et al., 2019; Yong et al., 2019). Recent studies have also reported a decrease in UV–vis light transmission after adding anthocyanins to biopolymer films (Alizadeh-Sani et al., 2021; Yong et al., 2019).

3.8. Total monomeric anthocyanins (TMA), total phenolic compounds (TPC), and antioxidant capacity

The results of total phenolic content (TPC), antioxidant activity (DPPH), and total monomeric anthocyanins (TMA) for the microparticles, HM-based films, and their composites (HM/IN/HAE, HM/MD/HAE, and HM/IN/MD/HAE) are presented in Table S2 and Fig. 7, respectively.

Hibiscus calyx extract (HAE) presented anthocyanins (TMA) contents of 192 mg/100 g and total phenolic compounds (TPC) contents of 23.5 mg GAE g^{-1}). As for antioxidant activity, HAE extract showed 18.2 mg TEAC g^{-1}. These values are in agreement with Liu, Zhang, Fu, & Cui, (2022) and Zhen et al., (2016). The HM films, as reported in other studies (Soultani, Evageliou, Koutelidakis, Kapsokefalou, & Komaitis, 2014), showed no antioxidant activity, and thus was not represented in Fig. 7. In contrast, films incorporated with HAE microparticles showed antioxidant and phenolic compounds. Kim, Yang, Lee, Beak, & Song, (2017) and Sáyago-Ayerdi, Velázquez-López, Montalvo-González, & Goñi, (2014) stated that dietary plant extract, such as that of hibiscus (HAE), have different bioactive compounds, such as vitamins (Vitamin C, Vitamin B1, and Vitamin B2), minerals (sodium, calcium, and potassium), and polyphenols (anthocyanins and carotenoids), acting as antioxidants. Also, there are many phenolic compounds in HAE, such as delphidin-3-sambubioside, cyanidin-3-sambubioside, quercetin, luteolin glycoside, and chlorogenic acid (Sáyago-Ayerdi et al., 2014).

Thus, the increase in antioxidant compounds was proportional to the 1:1 ratio and 20 % w/w concentration in the addition of IN/HAE, MD/HAE, and IN/MD/HAE microparticles. Gómez-Estaca, Bravo, Gómez-Guillén, Alemán, & Montero, (2009) reported that the biodegradable films' antioxidant activity is linked to the amount of antioxidant additives added, which agrees with the current study. This was observed that HM-based films added with MD/HAE microparticles showed higher antioxidant activity and total phenolic content. The HM/MD/HAE 1:1:20 films showed the highest phenolic compounds (20 mg GAE g^{-1}) and DPPH (11 mg TEAC g^{-1}) content. It was probably due to the antioxidant activity present in the HAE extract, as shown in Table S2, and in other studies (Cruz-Gálvez et al., 2018; de Moura et al., 2019; H. Kim et al., 2017; Peralta et al., 2019). Moreover, the higher antioxidant activity of biodegradable films added with MD microparticles may be linked to their good protection against oxidation and better storage stability. Chranioti, Nikoloudaki, & Tzia, (2015) and Chranioti & Tzia, (2014) showed similar observations. According to Vasco, Ruales, & Kamal-Eldin, (2008) foods may be classified into three levels as per their phenolics concentration: low (0.21 to 0.91 mg GAE.g^{-1}), intermediate (0.92 to 10.1 mg GAE.g^{-1}), and high (above 10.1 mg GAE.g^{-1}). Taking this classification into account, it was found that films incorporated with IN/HAE, MD/HAE, and IN/MD/HAE microparticles at 1:1 ratio and 20 % concentration may be classified as high content in phenolic compounds. Conversely, the other films may be seen as intermediate (Fig. 7).

3.9. Color stability of films

As one of the possible uses of these colorimetric films produced in our work is for the detection of the freshness of foods, such as meat and milk products, based on the color change of the film, it is necessary to characterize these modifications as a function of the variation of the pH (3,4,7 and 10). Table 5 shows the color changes of HM films and their composites (HM/IN/HAE, HM/MD/HAE, and HM/IN/MD/HAE) under different pH conditions. In this study, we sought to evaluate the color changes of the colorimetric films produced, simulating a more sensitive and objective measurement of color, using a calorimeter, since its measurement method is basically the same as that of the human eye, as established in other studies (Choi et al., 2017; Koshy et al., 2021; Jialin Liu et al., 2021; Ma, Du, et al., 2017; Teixeira, Soares, & Stringheta, 2021; Z. Yang et al., 2021; Zhai et al., 2017).

The results in Table 5 show that L^*, a^* and b^* values and the overall color difference (ΔE^*) of HM films did not change significantly with the 3–10 pH variation. This was verified with L^* values for HM/IN/HAE, HM/MD/HAE, and HM/IN/MD/HAE composite films incorporated with HAE extract microparticles, regardless of the wall material used to encapsulate it. However, a^* and b^* parameters varied significantly as a function of pH value, as observed in Table 5. The a^* values decreased with the increase in pH from 3 to 10, indicating a gradual loss of red coloration. The color changes of the films can be explained by the interactions of the chromophore nucleus of the anthocyanin with the H + concentration of the solutions. Chemically, anthocyanins can be defined as heterosides of an aglycone unit (anthocyanidins) linked to glycosides. With only one chromophore the flavylium nucleus, these pigments can

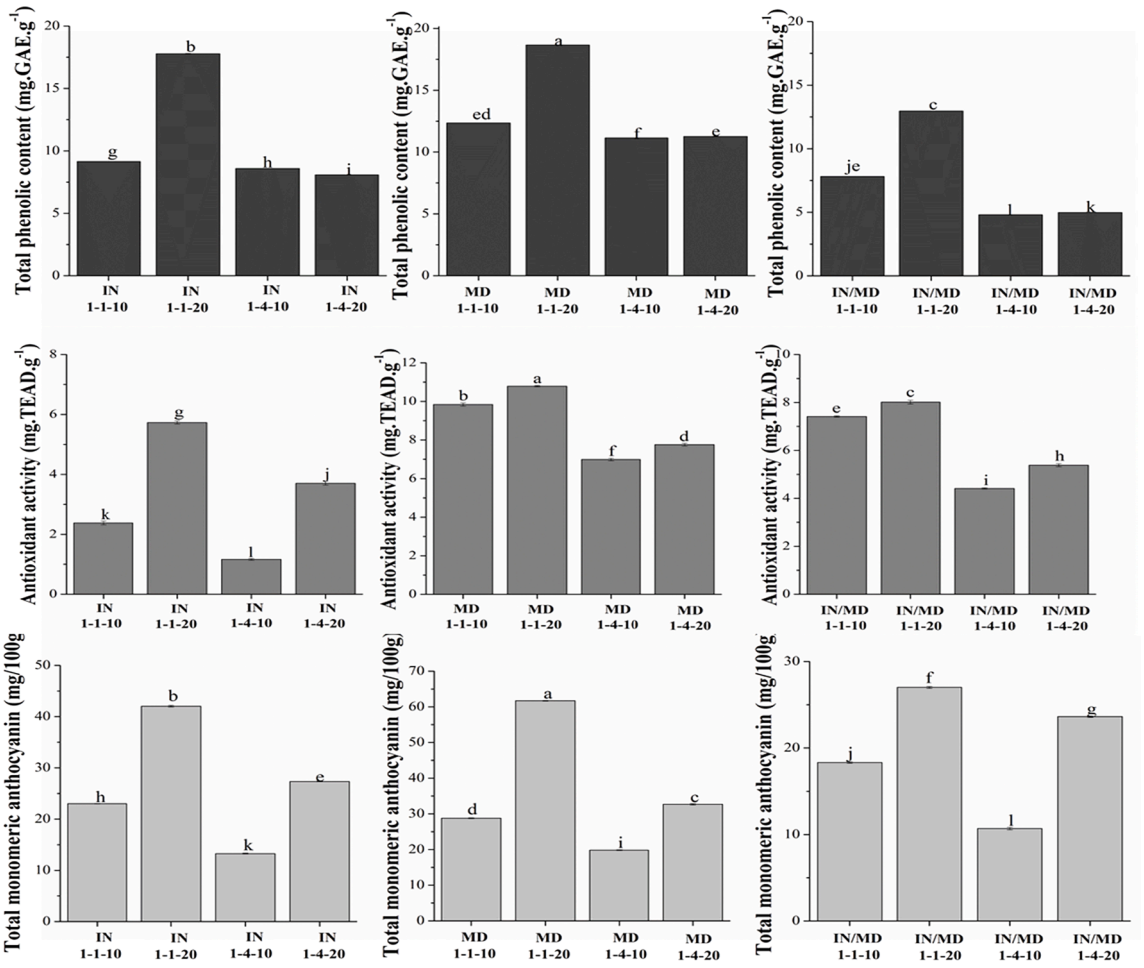

Fig. 7. Total phenolic content and antioxidant activity pectin (HM) films and pectin (HM)-based films and encapsulated anthocyanin powders with different wall materials: inulin (IN, a); maltodextrin (MD, b) and the inulin/maltodextrin combination (IN/MD, c), at different ratios (1: 1 and 1: 4) and concentrations (10 and 20%) added in the films.

provide a large range of colors, due to their interactions with compounds existing in aqueous medium. When raising the pH of an acid solution containing an anthocyanin, an acid-base protonation balance of the flavylium cation occurs very fast. The flavylium cation (AH +) is the predominant species in the equilibrium under strongly acidic conditions. With an increase in pH, AH + undergoes two parallel reactions: deprotonation, followed by proton loss, to give the hemiketal. Interconversion of these species produces large changes in color and stability. The colored species are AH+ (red), at low pH values, and A (purple/blue), which is not thermodynamically stable. These reactions lead to a structural configuration of anthocyanins in which, as the pH increases, decreases the number of conjugated double bonds and this characterizes the loss of coloration due to the pyrylium ring cleavage (Grajeda-Iglesias et al., 2016; Tarone et al., 2020). Table 5 shows that such reduction was greater in HM/IN/MD/HAE films added with HAE microparticles containing two wall materials, IN and MD. This may be related to better HAE extract encapsulation, corroborating with the studies of Calliari, Campardelli, Pettinato, & Perego, (2020), de Moura et al., (2019) and de Moura, Berling, Germer, Alvim, & Hubinger, (2018). Furthermore, at acidic pH (3–4), a^* parameters were observed with values above zero, which indicates a reddish-pink coloration. A similar analysis for the b^* parameter showed values above zero (yellowish color) and below (blue color tendency) for films with 20 % and 10 % HAE microparticle concentration, respectively. According to Etxabide, Kilmartin, & Maté, (2021) the color intensity decreases as the extract's concentration decreases. As for color difference (ΔE^*), ΔE between pH 3–4 and pH 7–10 were higher than 5, which indicates that color differences may be identified with the naked eye (H.-J. Kim, Roy, & Rhim, 2022; Koshy et al., 2021; Pourjavaher et al., 2017). Some more recent studies have used colorimetric films, similar to those developed in this study, to determine the quality and shelf life of certain foods (Hashim et al., 2022; D. Liu, Cui, Shang, & Zhong, 2021; Z. Yang et al., 2021; Zheng et al., 2022).

4. Conclusion

It has been demonstrated in the current study that incorporating anthocyanins-HAE microparticles by spray-drying with two encapsulating agents (MD and IN) at different concentrations to the HM-based films affected their matrices, giving them active functionality, preserving, and even improving their physicochemical properties. The incorporation of HAE microparticles in the HM matrix allowed the films to present antioxidant activity, which could also be considered as active films. Colorimetric films showed improved mechanical properties and barrier properties. To sum up, their application as intelligent packaging was highlighted, presenting coloration changes according to the different pH, further increasing their potential application in the food industry. All the materials used to fabricate the colorimetric films were nontoxic and biodegradable. Hence, the colorimetric films can be used as safe and eco-friendly fish, shrimp, pork, or milk indicators for intelligent packaging.

Table 5
Luminosity (L^*), *chroma* a^*, *chroma* b^*, and global color difference (ΔE^*) of pectin (HM) films and pectin (HM)-based films and encapsulated anthocyanin powders with different wall materials: inulin (IN); maltodextrin and inulin/maltodextrin combination (IN/MD), at different ratios (1: 1 and 1: 4) and concentrations (10 and 20%) added to the films immersed in different pH conditions buffer (from 3 to 10).

Samples	*pH*	L^*	a^*	b^*	ΔE
HM	**3**	87.0 ± 0.2$^{ab(a)}$	−1.1 ± 0.1$^{b(f)}$	5.0 ± 0.1$^{a(a)}$	6.0 ± 0.2^{a} (e)
	4	87.0 ± 0.1$^{b(a)}$	−0.9 ± 0.1$^{a(h)}$	5.0 ± 0.1$^{a(a)}$	6.2 ± 0.2$^{a(f)}$
	7	87.0 ± 0.3$^{ab(a)}$	−1.0 ± 0.1$^{a(g)}$	5.0 ± 0.1$^{a(a)}$	6.0 ± 0.2$^{a(j)}$
	10	88.0 ± 0.4$^{a(a)}$	−1.1 ± 0.1$^{bgn(e)}$	5.1 ± 0.1^{a} (bc)	6.0 ± 0.3^{a} (g)
IN/HAE-1:1:10	**3**	76.0 ± 0.2$^{ab(cd)}$	14.4 ± 0.4^{a} (c)	−0.03 ± 0.05$^{b(e)}$	22.0 ± 0.4^{a} (c)
	4	72.0 ± 6.0$^{b(fg)}$	13 ± 0.1^{b} (cde)	−0.5 ± 0.1^{c} (ef)	22.0 ± 2.0^{a} (c)
	7	77.0 ± 0.7$^{ab(cde)}$	12.4 ± 0.8^{c} (de)	0.5 ± 0.1$^{a(d)}$	20.0 ± 1.0^{a} (efg)
	10	80.0 ± 1.2$^{a(abc)}$	9.1 ± 1.4^{d} (bcd)	0.7 ± 0.2^{a} (fgh)	16.0 ± 2.0^{b} (de)
IN/HAE-1:1:20	**3**	65.0 ± 0.9$^{b(f)}$	31.0 ± 1.0^{a} (a)	−3.7 ± 0.2^{b} (h)	42.0 ± 1.0^{b} (a)
	4	64.0 ± 0.8$^{b(h)}$	30.0 ± 1.2^{a} (a)	−5.0 ± 0.4^{c} (hi)	42.0 ± 1.3^{b} (a)
	7	67.0 ± 2.2$^{b(h)}$	26.0 ± 4.0^{a} (ab)	−3.1 ± 0.6^{b} (f)	36.0 ± 4.0^{b} (ab)
	10	71.0 ± 2.0$^{a(cd)}$	16.0 ± 4.0^{b} (b)	−2.1 ± 0.7^{a} (i)	26.0 ± 3.0^{a} (b)
IN/HAE-1:4:10	**3**	81.0 ± 0.9$^{a(c)}$	8.0 ± 1.0^{a} (d)	2.0 ± 0.1^{bc} (c)	14.0 ± 1.0$^{ab(d)}$
	4	81.0 ± 1.0$^{a(bc)}$	8.0 ± 0.9^{a} (f)	2.0 ± 0.2$^{c(c)}$	14.0 ± 1.0^{a} (ef)
	7	81.0 ± 0.5$^{a(b)}$	7.0 ± 0.7^{a} (f)	2.4 ± 0.2^{b} (b)	13.0 ± 0.9$^{ab(hi)}$
	10	84.0 ± 3.0$^{a(a)}$	9.0 ± 4.0^{a} (bcd)	3.2 ± 0.4^{a} (bcdef)	10.0 ± 0.9^{b} (defg)
IN/HAE-1:4:20	**3**	74.0 ± 0.7$^{b(d)}$	17.0 ± 1.1^{b} (c)	−0.5 ± 0.1^{b} (f)	25.0 ± 1.4^{b} (c)
	4	75.0 ± 1.0^{c} (def)	15.0 ± 1.5^{a} (c)	−1.5 ± 0.1^{c} (f)	23.0 ± 2.0^{a} (c)
	7	75.0 ± 1.2$^{b(e)}$	15.0 ± 1.4^{b} (d)	−1.5 ± 0.1^{b} (e)	23.0 ± 2.0^{b} (e)
	10	80.0 ± 1.8$^{a(abc)}$	5.3 ± 1.4^{c} (cde)	2.0 ± 0.8^{a} (defg)	13.0 ± 2.0^{c} (def)
MD/HAE-1:1:10	**3**	77.0 ± 0.5^{c} (d)	14.0 ± 0.7^{a} (c)	−0.5 ± 0.1^{d} (f)	21.0 ± 0.8^{a} (c)
	4	76.0 ± 0.8$^{b(cde)}$	14.0 ± 1.2^{b} (cd)	−0.8 ± 0.1^{c} (ef)	21.0 ± 1.4^{b} (cd)
	7	78.0 ± 0.4$^{b(de)}$	11.0 ± 0.8^{b} (d)	1.1 ± 0.1^{b} (d)	17.0 ± 0.7^{b} (ef)
	10	80.0 ± 1.9$^{a(abc)}$	5.0 ± 4.0^{c} (cde)	2.3 ± 0.6^{a} (cdefg)	14.0 ± 4.0^{c} (def)
MD/HAE-1:1:20	**3**	65.0 ± 0.9$^{a(f)}$	31.0 ± 1.0^{b} (a)	−3.8 ± 0.2^{b} (h)	42.0 ± 1.4^{b} (a)
	4	66.0 ± 1.1$^{a(gh)}$	27.0 ± 2.0^{b} (a)	−5.4 ± 0.7^{b} (i)	38.0 ± 2.0^{b} (a)
	7	66.0 ± 1.2$^{a(h)}$	27.0 ± 2.0^{b} (a)	−5.4 ± 0.7^{b} (g)	38.0 ± 2.0^{b} (a)
	10	72.0 ± 2.0$^{a(cd)}$	14.0 ± 5.4^{a} (bc)	−1.6 ± 0.9^{a} (hi)	24.0 ± 5.0^{a} (bc)
MD/HAE-1:4:10	**3**	79.0 ± 2.0$^{a(c)}$	9.5 ± 3.0^{a} (d)	1.0 ± 0.2$^{a(d)}$	16.0 ± 3.5^{a} (d)
	4	78.0 ± 1.0$^{a(cd)}$	11.0 ± 2.0^{a} (def)	0.10 ± 0.01$^{a(de)}$	18.0 ± 2.0^{a} (de)
	7	79.0 ± 0.3$^{a(bcd)}$	11.0 ± 0.7^{a} (def)	1.1 ± 0.1^{a} (cd)	17.0 ± 0.7^{a} (fgh)
	10	79.0 ± 1.4$^{a(abc)}$	9.0 ± 4.0^{a} (bcd)	1.3 ± 0.9^{a} (efg)	16.0 ± 3.0^{a} (de)
MD/HAE-1:4:20	**3**	67.0 ± 0.4$^{a(e)}$	22.0 ± 3.0^{b} (b)	−4.0 ± 0.1^{b} (h)	34.0 ± 2.0^{b} (b)
	4	69.0 ± 1.7$^{a(gh)}$	22.0 ± 1.4^{b} (b)	−4.0 ± 0.6^{b} (h)	32.0 ± 2.3^{b} (b)
	7	69.4 ± 1.7$^{a(fg)}$	22.0 ± 1.4^{b} (bc)	−4.0 ± 0.6^{b} (f)	32.0 ± 2.3^{b} (cd)
	10	65.0 ± 9.0$^{a(d)}$	60.0 ± 3.0^{a} (a)	63.0 ± 2.0^{a} (a)	93.0 ± 3.0^{a} (a)
IN/MD/HAE-1:1:10	**3**	79.0 ± 0.4$^{b(c)}$	10.0 ± 0.5$^{(d)}$	1.4 ± 0.1^{bc} (d)	17.0 ± 0.6$^{(d)}$
	4	79.0 ± 0.6$^{b(bcd)}$	10.0 ± 0.2$^{(ef)}$	1.0 ± 0.3^{c} (cd)	17.0 ± 0.5$^{(e)}$
	7	80.0 ± 0.5$^{b(bc)}$	8.3 ± 0.9$^{(ef)}$	2.3 ± 0.5^{b} (bc)	15.0 ± 0.9$^{(gh)}$
	10	85.0 ± 2.0$^{a(ab)}$	1.2 ± 0.1$^{(de)}$	3.5 ± 0.5^{a} (bcde)	9.0 ± 1.3$^{(efg)}$
IN/MD/HAE-1:1:20	**3**	75.0 ± 0.2$^{a(cd)}$	14.0 ± 0.9^{c} (c)	−1.3 ± 0.1^{b} (g)	22.0 ± 0.8^{b} (c)
	4	71.0 ± 1.2$^{b(efg)}$	20.4 ± 1.5^{a} (b)	−2.8 ± 0.4^{c} (g)	30.0 ± 1.8^{a} (b)
	7	71.0 ± 1.2$^{b(f)}$	20.4 ± 1.4^{a} (c)	−2.8 ± 0.4^{c} (f)	30.0 ± 1.8^{a} (d)
	10	77.0 ± 0.6$^{a(bc)}$	9.0 ± 1.1^{d} (bcd)	0.1 ± 0.0^{a} (ghi)	18.0 ± 1.1^{b} (cd)
IN/MD/HAE-1:4:10	**3**	84.0 ± 0.3$^{a(b)}$	3.6 ± 0.2^{a} (e)	3.4 ± 0.1^{bc} (b)	10.0 ± 0.4^{a} (e)
	4	83.0 ± 0.6$^{a(ab)}$	3.5 ± 0.3^{a} (g)	3.2 ± 0.2$^{c(b)}$	9.5 ± 0.7$^{a(f)}$
	7	85.0 ± 0.9$^{a(a)}$	2.5 ± 0.3^{b} (fg)	4.0 ± 0.4^{ab} (a)	8.3 ± 0.9^{ab} (ij)
	10	85.0 ± 2.1$^{a(ab)}$	1.2 ± 0.1^{c} (de)	3.5 ± 0.5^{a} (bcd)	8.8 ± 1.3^{a} (fg)
IN/MD/HAE-1:4:20	**3**	80.0 ± 0.3$^{b(c)}$	9.5 ± 0.4^{a} (d)	1.2 ± 0.0^{b} (d)	16.0 ± 0.5^{a} (d)
	4	79.5 ± 0.7$^{b(bcd)}$	9.4 ± 0.9^{a} (f)	0.8 ± 0.1^{b} (cd)	16.0 ± 1.1^{a} (e)
	7	80.0 ± 0.5$^{ab(bc)}$	8.2 ± 0.5^{a} (ef)	1.7 ± 0.1^{b} (bc)	14.5 ± 0.7^{a} (gh)
	10	82.0 ± 1.1$^{a(ab)}$	−1.1 ± 0.1$^{b(e)}$	6.0 ± 2.0$^{a(b)}$	11.2 ± 2.0^{b} (defg)

Different letters within the same treatment (without parentheses) and between treatments (in parentheses) indicated statistically significant differences ($p < 0.05$) by Tukey's test.

CRediT authorship contribution statement

Juliana Farinassi Mendes: Conceptualization, Methodology, Formal analysis, Investigation, Writing – original draft. **Laís Bruno Norcino:** Formal analysis, Investigation. **Anny Manrich:** Resources, Writing – review & editing. **Tiago José Pires de Oliveira:** Supervision, Conceptualization, Methodology, Writing – review & editing. **Rafael Farinassi Mendes:** Supervision, Conceptualization, Methodology, Writing – review & editing. **Luiz Henrique Capparelli Mattoso:** Supervision, Conceptualization, Methodology, Writing – review & editing.

Declaration of Competing Interest

The authors declare that they have no known competing financial interests or personal relationships that could have appeared to influence the work reported in this paper.

Acknowledgments

The authors would like to thank the National Council for Scientific and Technological Development – CNPq (grant #305662/2020-1), FAPESP (grant #2019/26622-4), CAPES, and the Brazilian Agricultural Research Corporation (Embrapa), in particular Embrapa Instrumentação, for their support.

Appendix A. Supplementary material

Supplementary data to this article can be found online at https://doi.org/10.1016/j.foodres.2022.111914.

References

Figueiredo, J. A., MT Lago, A., Mar, J. M., Silva, L. S., Sanches, E., Souza, T. P., … Borges, S. V. (2020). Stability of camu-camu encapsulated with different prebiotic biopolymers. *Journal of the Science of Food and Agriculture, 100*(8), 3471–3480. https://doi.org/10.1002/jsfa.10384

Abdelghany, A. M., Menazea, A. A., & Ismail, A. M. (2019). Synthesis, characterization and antimicrobial activity of Chitosan/Polyvinyl Alcohol blend doped with Hibiscus Sabdariffa L. extract. *Journal of Molecular Structure, 1197*, 603–609. https://doi.org/10.1016/j.molstruc.2019.07.089

Abral, H., Basri, A., Muhammad, F., Fernando, Y., Hafizulhaq, F., Mahardika, M., … Stephane, I. (2019). A simple method for improving the properties of the sago starch films prepared by using ultrasonication treatment. *Food Hydrocolloids, 93*, 276–283. https://doi.org/10.1016/j.foodhyd.2019.02.012

Agarwal, S. (2021). Major factors affecting the characteristics of starch based biopolymer films. *European Polymer Journal, 160*, Article 110788. https://doi.org/10.1016/j.eurpolymj.2021.110788

Akhavan Mahdavi, S., Jafari, S. M., Assadpoor, E., & Dehnad, D. (2016). Microencapsulation optimization of natural anthocyanins with maltodextrin, gum Arabic and gelatin. *International Journal of Biological Macromolecules, 85*, 379–385. https://doi.org/10.1016/j.ijbiomac.2016.01.011

Alamri, H., & Low, I. M. (2010). Characterization and Properties of Recycled Cellulose Fibre- Reinforced Epoxy-Hybrid Clay Nanocomposites. *Materials Science Forum, 654–656*, 2624–2627. https://doi.org/10.4028/www.scientific.net/MSF.654-656.2624

Alizadeh-Sani, M., Tavassoli, M., Mohammadian, E., Ehsani, A., Khaniki, G. J., Priyadarshi, R., & Rhim, J.-W. (2021). pH-responsive color indicator films based on methylcellulose/chitosan nanofiber and barberry anthocyanins for real-time monitoring of meat freshness. *International Journal of Biological Macromolecules, 166*, 741–750. https://doi.org/10.1016/j.ijbiomac.2020.10.231

Almasi, H., Azizi, S., & Amjadi, S. (2020). Development and characterization of pectin films activated by nanoemulsion and Pickering emulsion stabilized marjoram (Origanum majorana L.) essential oil. *Food Hydrocolloids, 99*, Article 105338. https://doi.org/10.1016/j.foodhyd.2019.105338

Aoac. (2006). *Official Methods of Analysis* (14th ed.). Washington, USA: Ass. Off. Analytical. Chem.

Araujo-Díaz, S. B., Leyva-Porras, C., Aguirre-Bañuelos, P., Álvarez-Salas, C., & Saavedra-Leos, Z. (2017). Evaluation of the physical properties and conservation of the antioxidants content, employing inulin and maltodextrin in the spray drying of blueberry juice. *Carbohydrate Polymers, 167*, 317–325. https://doi.org/10.1016/j.carbpol.2017.03.065

Araujo-Farro, P. C., Podadera, G., Sobral, P. J. A., & Menegalli, F. C. (2010). Development of films based on quinoa (Chenopodium quinoa, Willdenow) starch. *Carbohydrate Polymers, 81*(4), 839–848. https://doi.org/10.1016/j.carbpol.2010.03.051

ASTM D882-09. (2009). *Standard Test Method for Tensile Properties of Thin Plastic Sheeting.* PA: West Conshohocken.

ASTM E96. (2016). Standard Test Methods for Water Vapor Transmission of Materials.

Azeredo, H. M. C., Morrugares-Carmona, R., Wellner, N., Cross, K., Bajka, B., & Waldron, K. W. (2016). Development of pectin films with pomegranate juice and citric acid. *Food Chemistry, 198*, 101–106. https://doi.org/10.1016/j.foodchem.2015.10.117

Basiak, E., Lenart, A., & Debeaufort, F. (2017). Effect of starch type on the physico-chemical properties of edible films. *International Journal of Biological Macromolecules, 98*, 348–356. https://doi.org/10.1016/j.ijbiomac.2017.01.122

Bedane, A. H., Eić, M., Farmahini-Farahani, M., & Xiao, H. (2015). Water vapor transport properties of regenerated cellulose and nanofibrillated cellulose films. *Journal of Membrane Science, 493*, 46–57. https://doi.org/10.1016/j.memsci.2015.06.009

Brand-Williams, W., Cuvelier, M. E., & Berset, C. (1995). Use of a free radical method to evaluate antioxidant activity. *LWT - Food Science and Technology, 28*(1), 25–30. https://doi.org/10.1016/S0023-6438(95)80008-5

Calliari, C. M., Campardelli, R., Pettinato, M., & Perego, P. (2020). Encapsulation of Hibiscus sabdariffa Extract into Zein Nanoparticles. *Chemical Engineering & Technology, 43*(10), 2062–2072. https://doi.org/10.1002/ceat.202000194

Carmo, E. L., Teodoro, R. A. R., Campelo, P. H., Figueiredo, J. de A., Botrel, D. A., Fernandes, R. V. de B., & Borges, S. V. (2019). The use of different temperatures and inulin: Whey protein isolate ratios in the spray drying of beetroot juice. *Journal of Food Processing and Preservation, 43*(10). https://doi.org/10.1111/jfpp.14113.

Cheng, H., Wu, W., Chen, J., Pan, H., Xu, E., Chen, S., … Chen, J. (2022). Establishment of anthocyanin fingerprint in black wolfberry fruit for quality and geographical origin identification. *LWT, 157*, Article 113080. https://doi.org/10.1016/j.lwt.2022.113080

Choi, I., Lee, J. Y., Lacroix, M., & Han, J. (2017). Intelligent pH indicator film composed of agar/potato starch and anthocyanin extracts from purple sweet potato. *Food Chemistry, 218*, 122–128. https://doi.org/10.1016/j.foodchem.2016.09.050

Chranioti, C., Nikoloudaki, A., & Tzia, C. (2015). Saffron and beetroot extracts encapsulated in maltodextrin, gum Arabic, modified starch and chitosan: Incorporation in a chewing gum system. *Carbohydrate Polymers, 127*, 252–263. https://doi.org/10.1016/j.carbpol.2015.03.049

Chranioti, C., & Tzia, C. (2014). Thermooxidative Stability of Fennel Oleoresin Microencapsulated in Blended Biopolymer Agents. *Journal of Food Science, 79*(6), C1091–C1099. https://doi.org/10.1111/1750-3841.12474

Cruz-Gálvez, A. M., Castro-Rosas, J., Rodríguez-Marín, M. L., Cadena-Ramírez, A., Tellez-Jurado, A., Tovar-Jiménez, X., … Gómez-Aldapa, C. A. (2018). Antimicrobial activity and physicochemical characterization of a potato starch-based film containing acetonic and methanolic extracts of Hibiscus sabdariffa for use in sausage. *LWT, 93*, 300–305. https://doi.org/10.1016/j.lwt.2018.02.064

da Silva Carvalho, A. G., da Costa Machado, M. T., da Silva, V. M., Sartoratto, A., Rodrigues, R. A. F., & Hubinger, M. D. (2016). Physical properties and morphology of spray dried microparticles containing anthocyanins of jussara (Euterpe edulis Martius) extract. *Powder Technology, 294*, 421–428. https://doi.org/10.1016/j.powtec.2016.03.007

da Silveira, T. F. F., Cristianini, M., Kuhnle, G. G., Ribeiro, A. B., Filho, J. T., & Godoy, H. T. (2019). Anthocyanins, non-anthocyanin phenolics, tocopherols and antioxidant capacity of açaí juice (Euterpe oleracea) as affected by high pressure processing and thermal pasteurization. *Innovative Food Science & Emerging Technologies, 55*, 88–96. https://doi.org/10.1016/j.ifset.2019.05.001

de Moura, S. C. S. R., Berling, C. L., Garcia, A. O., Queiroz, M. B., Alvim, I. D., & Hubinger, M. D. (2019). Release of anthocyanins from the hibiscus extract encapsulated by ionic gelation and application of microparticles in jelly candy. *Food Research International, 121*, 542–552. https://doi.org/10.1016/j.foodres.2018.12.010

de Moura, S. C. S. R., Berling, C. L., Germer, S. P. M., Alvim, I. D., & Hubinger, M. D. (2018). Encapsulating anthocyanins from Hibiscus sabdariffa L. calyces by ionic gelation: Pigment stability during storage of microparticles. *Food Chemistry, 241*, 317–327. https://doi.org/10.1016/j.foodchem.2017.08.095

Degenhardt, A., Knapp, H., & Winterhalter, P. (2000). Separation and Purification of Anthocyanins by High-Speed Countercurrent Chromatography and Screening for Antioxidant Activity. *Journal of Agricultural and Food Chemistry, 48*(2), 338–343. https://doi.org/10.1021/jf990876t

Deng, Q., & Zhao, Y. (2011). Physicochemical, Nutritional, and Antimicrobial Properties of Wine Grape (cv. Merlot) Pomace Extract-Based Films. *Journal of Food Science, 76*(3), E309–E317. https://doi.org/10.1111/j.1750-3841.2011.02090.x

Duncan, S. E., & Chang, H.-H. (2012). Implications of Light Energy on Food Quality and Packaging Selection (pp. 25–73). https://doi.org/10.1016/B978-0-12-394598-3.00002-2.

Eça, K. S., Machado, M. T. C., Hubinger, M. D., & Menegalli, F. C. (2015). Development of Active Films From Pectin and Fruit Extracts: Light Protection, Antioxidant Capacity, and Compounds Stability. *Journal of Food Science, 80*(11), C2389–C2396. https://doi.org/10.1111/1750-3841.13074

Etxabide, A., Kilmartin, P. A., & Maté, J. I. (2021). Color stability and pH-indicator ability of curcumin, anthocyanin and betanin containing colorants under different storage conditions for intelligent packaging development. *Food Control, 121*, Article 107645. https://doi.org/10.1016/j.foodcont.2020.107645

Etxabide, A., Maté, J. I., & Kilmartin, P. A. (2021). Effect of curcumin, betanin and anthocyanin containing colourants addition on gelatin films properties for intelligent films development. *Food Hydrocolloids, 115*, Article 106593. https://doi.org/10.1016/j.foodhyd.2021.106593

Fernandes, R. V. de B., Borges, S. V., & Botrel, D. A. (2014). Gum arabic/starch/maltodextrin/inulin as wall materials on the microencapsulation of rosemary essential oil. *Carbohydrate Polymers, 101*, 524–532. https://doi.org/10.1016/j.carbpol.2013.09.083.

Fernandes, R. V. de B., Silva, E. K., Borges, S. V., de Oliveira, C. R., Yoshida, M. I., da Silva, Y. F., … Botrel, D. A. (2017). Proposing Novel Encapsulating Matrices for Spray-Dried Ginger Essential Oil from the Whey Protein Isolate-Inulin/Maltodextrin Blends. *Food and Bioprocess Technology, 10*(1), 115–130. https://doi.org/10.1007/s11947-016-1803-1.

Fraga, C. G., Galleano, M., Verstraeten, S. V., & Oteiza, P. I. (2010). Basic biochemical mechanisms behind the health benefits of polyphenols. *Molecular Aspects of Medicine, 31*(6), 435–445. https://doi.org/10.1016/j.mam.2010.09.006

Franco, G. T., Otoni, C. G., Lodi, B. D., Lorevice, M. V., de Moura, M. R., & Mattoso, L. H. C. (2020). Escalating the technical bounds for the production of cellulose-aided peach leathers: From the benchtop to the pilot plant. *Carbohydrate Polymers, 245*, Article 116437. https://doi.org/10.1016/j.carbpol.2020.116437

Galus, S. (2018). Functional properties of soy protein isolate edible films as affected by rapeseed oil concentration. *Food Hydrocolloids, 85*, 233–241. https://doi.org/10.1016/j.foodhyd.2018.07.026

Gharsallaoui, A., Saurel, R., Chambin, O., & Voilley, A. (2012). Pea (Pisum sativum, L.) Protein Isolate Stabilized Emulsions: A Novel System for Microencapsulation of Lipophilic Ingredients by Spray Drying. *Food and Bioprocess Technology, 5*(6), 2211–2221. https://doi.org/10.1007/s11947-010-0497-z

Giusti, M. M., & Wrolstad, R. E. (2001). Characterization and Measurement of Anthocyanins by UV-Visible Spectroscopy. *Current Protocols in Food. Analytical Chemistry, 00*(1). https://doi.org/10.1002/0471142913.faf0102s00

Gómez-Estaca, J., Bravo, L., Gómez-Guillén, M. C., Alemán, A., & Montero, P. (2009). Antioxidant properties of tuna-skin and bovine-hide gelatin films induced by the addition of oregano and rosemary extracts. *Food Chemistry, 112*(1), 18–25. https://doi.org/10.1016/j.foodchem.2008.05.034

Gouveia, T. I. A., Biernacki, K., Castro, M. C. R., Gonçalves, M. P., & Souza, H. K. S. (2019). A new approach to develop biodegradable films based on thermoplastic pectin. *Food Hydrocolloids, 97*, Article 105175. https://doi.org/10.1016/j.foodhyd.2019.105175

Grajeda-Iglesias, C., Figueroa-Espinoza, M. C., Barouh, N., Baréa, B., Fernandes, A., de Freitas, V., & Salas, E. (2016). Isolation and Characterization of Anthocyanins from Hibiscus sabdariffa Flowers. *Journal of Natural Products, 79*(7), 1709–1718. https://doi.org/10.1021/acs.jnatprod.5b00958

Guo, Z., Ge, X., Li, W., Yang, L., Han, L., & Yu, Q. (2021). Active-intelligent film based on pectin from watermelon peel containing beetroot extract to monitor the freshness of packaged chilled beef. *Food Hydrocolloids, 106751*. https://doi.org/10.1016/j.foodhyd.2021.106751

Hashim, S. B. H., Elrasheid Tahir, H., Liu, L., Zhang, J., Zhai, X., Ali Mahdi, A., … Jiyong, S. (2022). Intelligent colorimetric pH sensoring packaging films based on sugarcane wax/agar integrated with butterfly pea flower extract for optical tracking of shrimp freshness. *Food Chemistry, 373*, Article 131514. https://doi.org/10.1016/j.foodchem.2021.131514

Huang, S., Xiong, Y., Zou, Y., Dong, Q., Ding, F., Liu, X., & Li, H. (2019). A novel colorimetric indicator based on agar incorporated with Arnebia euchroma root extracts for monitoring fish freshness. *Food Hydrocolloids, 90*, 198–205. https://doi.org/10.1016/j.foodhyd.2018.12.009

Jamróz, E., Tkaczewska, J., Juszczak, L., Zimowska, M., Kawecka, A., Krzyściak, P., & Skóra, M. (2022). The influence of lingonberry extract on the properties of novel, double-layered biopolymer films based on furcellaran, CMC and a gelatin hydrolysate. *Food Hydrocolloids, 124*, Article 107334. https://doi.org/10.1016/j.foodhyd.2021.107334

Jiang, G., Hou, X., Zeng, X., Zhang, C., Wu, H., Shen, G., … Zhang, Z. (2020). Preparation and characterization of indicator films from carboxymethyl-cellulose/starch and purple sweet potato (Ipomoea batatas (L.) lam) anthocyanins for monitoring fish freshness. *International Journal of Biological Macromolecules, 143*, 359–372. https://doi.org/10.1016/j.ijbiomac.2019.12.024

Jimenez-Gonzalez, O., Ruiz-Espinosa, H., Luna-Guevara, J. J., Ochoa-Velasco, C. E., Luna Vital, D., & Luna-Guevara, M. L. (2018). A potential natural coloring agent with antioxidant properties: Microencapsulates of Renealmia alpinia (Rottb.) Maas fruit pericarp. *NFS Journal, 13*, 1–9. https://doi.org/10.1016/j.nfs.2018.08.001

Jiménez, A., Fabra, M. J., Talens, P., & Chiralt, A. (2010). Effect of lipid self-association on the microstructure and physical properties of hydroxypropyl-methylcellulose edible films containing fatty acids. *Carbohydrate Polymers, 82*(3), 585–593. https://doi.org/10.1016/j.carbpol.2010.05.014

Kang, S., Wang, H., Guo, M., Zhang, L., Chen, M., Jiang, S., … Jiang, S. (2018). Ethylene-vinyl Alcohol Copolymer-Montmorillonite Multilayer Barrier Film Coated with Mulberry Anthocyanin for Freshness Monitoring. *Journal of Agricultural and Food Chemistry, 66*(50), 13268–13276. https://doi.org/10.1021/acs.jafc.8b05189

Kim, H.-J., Roy, S., & Rhim, J.-W. (2022). Gelatin/agar-based color-indicator film integrated with Clitoria ternatea flower anthocyanin and zinc oxide nanoparticles for monitoring freshness of shrimp. *Food Hydrocolloids, 124*, Article 107294. https://doi.org/10.1016/j.foodhyd.2021.107294

Kim, H., Yang, H.-J., Lee, K.-Y., Beak, S.-E., & Song, K. B. (2017). Characterization of red ginseng residue protein films incorporated with hibiscus extract. *Food Science and Biotechnology, 26*(2), 369–374. https://doi.org/10.1007/s10068-017-0050-1

Koosha, M., & Hamedi, S. (2019). Intelligent Chitosan/PVA nanocomposite films containing black carrot anthocyanin and bentonite nanoclays with improved mechanical, thermal and antibacterial properties. *Progress in Organic Coatings, 127*, 338–347. https://doi.org/10.1016/j.porgcoat.2018.11.028

Koshy, R. R., Koshy, J. T., Mary, S. K., Sadanandan, S., Jisha, S., & Pothan, L. A. (2021). Preparation of pH sensitive film based on starch/carbon nano dots incorporating anthocyanin for monitoring spoilage of pork. *Food Control, 126*, Article 108039. https://doi.org/10.1016/j.foodcont.2021.108039

Liu, D., Cui, Z., Shang, M., & Zhong, Y. (2021). A colorimetric film based on polyvinyl alcohol/sodium carboxymethyl cellulose incorporated with red cabbage anthocyanin for monitoring pork freshness. *Food Packaging and Shelf Life, 28*, Article 100641. https://doi.org/10.1016/j.fpsl.2021.100641

Liu, J.-Z., Zhang, C.-C., Fu, Y.-J., & Cui, Q. (2022). Comparative analysis of phytochemical profile, antioxidant and anti-inflammatory activity from Hibiscus manihot L. flower. *Arabian Journal of Chemistry, 15*(1), Article 103503. https://doi.org/10.1016/j.arabjc.2021.103503

Liu, J., Huang, J., Ying, Y., Hu, L., & Hu, Y. (2021). pH-sensitive and antibacterial films developed by incorporating anthocyanins extracted from purple potato or roselle into chitosan/polyvinyl alcohol/nano-ZnO matrix: Comparative study. *International Journal of Biological Macromolecules, 178*, 104–112. https://doi.org/10.1016/j.ijbiomac.2021.02.115

Liu, J., Wang, H., Guo, M., Li, L., Chen, M., Jiang, S., … Jiang, S. (2019). Extract from Lycium ruthenicum Murr. Incorporating κ-carrageenan colorimetric film with a wide pH–sensing range for food freshness monitoring. *Food Hydrocolloids, 94*, 1–10. https://doi.org/10.1016/j.foodhyd.2019.03.008

Liu, J., Wang, H., Wang, P., Guo, M., Jiang, S., Li, X., & Jiang, S. (2018). Films based on κ-carrageenan incorporated with curcumin for freshness monitoring. *Food Hydrocolloids, 83*, 134–142. https://doi.org/10.1016/j.foodhyd.2018.05.012

Luiza Koop, B., Nascimento da Silva, M., Diniz da Silva, F., dos Santos, T., Lima, K., Santos Soares, L., … Rodrigues Monteiro, A. (2022). Flavonoids, anthocyanins, betalains, curcumin, and carotenoids: Sources, classification and enhanced stabilization by encapsulation and adsorption. *Food Research International, 153*, Article 110929. https://doi.org/10.1016/j.foodres.2021.110929

Luo, Q., Hossen, A., Sameen, D. E., Ahmed, S., Dai, J., Li, S., … Liu, Y. (2021). Recent advances in the fabrication of pH-sensitive indicators films and their application for food quality evaluation. *Critical Reviews in Food Science and Nutrition, 1–17*. https://doi.org/10.1080/10408398.2021.1959296

Ma, Q., Du, L., & Wang, L. (2017). Tara gum/polyvinyl alcohol-based colorimetric NH3 indicator films incorporating curcumin for intelligent packaging. *Sensors and Actuators B: Chemical, 244*, 759–766. https://doi.org/10.1016/j.snb.2017.01.035

Ma, Q., Ren, Y., Gu, Z., & Wang, L. (2017). Developing an intelligent film containing Vitis amurensis husk extracts: The effects of pH value of the film-forming solution. *Journal of Cleaner Production, 166*, 851–859. https://doi.org/10.1016/j.jclepro.2017.08.099

Ma, Q., & Wang, L. (2016). Preparation of a visual pH-sensing film based on tara gum incorporating cellulose and extracts from grape skins. *Sensors and Actuators B: Chemical, 235*, 401–407. https://doi.org/10.1016/j.snb.2016.05.107

Maciel, L. G., do Carmo, M. A. V., Azevedo, L., Daguer, H., Molognoni, L., de Almeida, M. M., … Rosso, N. D. (2018). Hibiscus sabdariffa anthocyanins-rich extract: Chemical stability, in vitro antioxidant and antiproliferative activities. *Food and Chemical Toxicology, 113*, 187–197. https://doi.org/10.1016/j.fct.2018.01.053.

Maftoonazad, Neda Ramaswamy, H. S., & Marcotte, M. (2007). Evaluation of factors affecting barrier, mechanical and optical properties of pectin-based films using response surface methodology. *Journal of Food Process Engineering, 30*(5), 539–563. https://doi.org/10.1111/j.1745-4530.2007.00123.x.

Mandal, A., & Chakrabarty, D. (2019). Studies on mechanical, thermal, and barrier properties of carboxymethyl cellulose film highly filled with nanocellulose. *Journal of Thermoplastic Composite Materials, 32*(7), 995–1014. https://doi.org/10.1177/0892705718772868

Manrich, A., Moreira, F. K. V., Otoni, C. G., Lorevice, M. V., Martins, M. A., & Mattoso, L. H. C. (2017). Hydrophobic edible films made up of tomato cutin and pectin. *Carbohydrate Polymers, 164*, 83–91. https://doi.org/10.1016/j.carbpol.2017.01.075

Mar, J. M., da Silva, L. S., Lira, A. C., Kinupp, V. F., Yoshida, M. I., Moreira, W. P., … Sanches, E. A. (2020). Bioactive compounds-rich powders: Influence of different carriers and drying techniques on the chemical stability of the Hibiscus acetosella extract. *Powder Technology, 360*, 383–391. https://doi.org/10.1016/j.powtec.2019.10.062

Mehran, M., Masoum, S., & Memarzadeh, M. (2020). Improvement of thermal stability and antioxidant activity of anthocyanins of Echium amoenum petal using maltodextrin/modified starch combination as wall material. *International Journal of Biological Macromolecules, 148*, 768–776. https://doi.org/10.1016/j.ijbiomac.2020.01.197

Mendes, J. F., Martins, J. T., Manrich, A., Sena Neto, A. R., Pinheiro, A. C. M., Mattoso, L. H. C., & Martins, M. A. (2019a). Development and physical-chemical properties of pectin film reinforced with spent coffee grounds by continuous casting. *Carbohydrate Polymers, 210*, 92–99. https://doi.org/10.1016/j.carbpol.2019.01.058

Mendes, J. F., Martins, J. T., Manrich, A., Sena Neto, A. R., Pinheiro, A. C. M., Mattoso, L. H. C., & Martins, M. A. (2019b). Development and physical-chemical properties of pectin film reinforced with spent coffee grounds by continuous casting. *Carbohydrate Polymers, 210*. https://doi.org/10.1016/j.carbpol.2019.01.058

Mendes, J. F., Norcino, L. B., Manrich, A., Pinheiro, A. C. M., Oliveira, J. E., & Mattoso, L. H. C. (2020). Characterization of Pectin Films Integrated with Cocoa Butter by Continuous Casting: Physical, Thermal and Barrier Properties. *Journal of Polymers and the Environment, 28*(11), 2905–2917. https://doi.org/10.1007/s10924-020-01829-1

Mendes, J. F., Norcino, L. B., Martins, H. H. A., Manrich, A., Otoni, C. G., Carvalho, E. E. N., … Mattoso, L. H. C. (2020a). Correlating emulsion characteristics with the properties of active starch films loaded with lemongrass essential oil. *Food Hydrocolloids, 100*. https://doi.org/10.1016/j.foodhyd.2019.105428

Mendes, J. F., Norcino, L. B., Martins, H. H. A., Manrich, A., Otoni, C. G., Carvalho, E. E. N., … Mattoso, L. H. C. (2020b). Correlating emulsion characteristics with the properties of active starch films loaded with lemongrass essential oil. *Food Hydrocolloids, 100*, Article 105428. https://doi.org/10.1016/j.foodhyd.2019.105428

Milda E. Embuscado, K. C. H. (2009). *Edible Films and Coatings for Food Applications*. (K. C. Huber & M. E. Embuscado, Eds.). New York, NY: Springer New York. https://doi.org/10.1007/978-0-387-92824-1.

Miranda-Linares, V., Quintanar-Guerrero, D., Del Real, A., & Zambrano-Zaragoza, M. L. (2020). Spray-drying method for the encapsulation of a functionalized ingredient in alginate-pectin nano- and microparticles loaded with distinct natural actives: Stability and antioxidant effect. *Food Hydrocolloids, 101*, Article 105560. https://doi.org/10.1016/j.foodhyd.2019.105560

Moghbeli, S., Jafari, S. M., Maghsoudlou, Y., & Dehnad, D. (2019). Influence of pectin-whey protein complexes and surfactant on the yield and microstructural properties of date powder produced by spray drying. *Journal of Food Engineering, 242*, 124–132. https://doi.org/10.1016/j.jfoodeng.2018.08.025

Nayak, C. A., & Rastogi, N. K. (2010). Effect of Selected Additives on Microencapsulation of Anthocyanin by Spray Drying. *Drying Technology, 28*(12), 1396–1404. https://doi.org/10.1080/07373937.2010.482705

Nisar, T., Wang, Z.-C., Yang, X., Tian, Y., Iqbal, M., & Guo, Y. (2018). Characterization of citrus pectin films integrated with clove bud essential oil: Physical, thermal, barrier, antioxidant and antibacterial properties. *International Journal of Biological Macromolecules, 106*, 670–680. https://doi.org/10.1016/j.ijbiomac.2017.08.068

Nogueira, G. F., Fakhouri, F. M., Velasco, J. I., & de Oliveira, R. A. (2019). Active Edible Films Based on Arrowroot Starch with Microparticles of Blackberry Pulp Obtained by Freeze-Drying for Food Packaging. *Polymers, 11*(9), 1382. https://doi.org/10.3390/polym11091382

de Oliveira Filho, J. G., Braga, A. R. C., de Oliveira, B. R., Gomes, F. P., Moreira, V. L., Pereira, V. A. C., & Egea, M. B. (2021). The potential of anthocyanins in smart, active, and bioactive eco-friendly polymer-based films: A review. *Food Research International, 142*, Article 110202. https://doi.org/10.1016/j.foodres.2021.110202

Oun, A. A., & Rhim, J.-W. (2016). Isolation of cellulose nanocrystals from grain straws and their use for the preparation of carboxymethyl cellulose-based nanocomposite films. *Carbohydrate Polymers, 150*, 187–200. https://doi.org/10.1016/j.carbpol.2016.05.020

Chumsri, P., & Sirichote Anchalee, A. I. (2008). Studies on the optimum conditions for the extraction and concentration of roselle (Hibiscus sabdariffa Linn.) extract. *Songklanakarin Journal of Science and Technology, 30*, 133–139.

Pająk, P., Przetaczek-Rożnowska, I., & Juszczak, L. (2019). Development and physicochemical, thermal and mechanical properties of edible films based on pumpkin, lentil and quinoa starches. *International Journal of Biological Macromolecules, 138*, 441–449. https://doi.org/10.1016/j.ijbiomac.2019.07.074

Peralta, J., Bitencourt-Cervi, C. M., Maciel, V. B. V., Yoshida, C. M. P., & Carvalho, R. A. (2019). Aqueous hibiscus extract as a potential natural pH indicator incorporated in

natural polymeric films. *Food Packaging and Shelf Life, 19*, 47–55. https://doi.org/10.1016/j.fpsl.2018.11.017

Pereira Souza, A. C., Deyse Gurak, P., Marczak, D. F., & L.. (2017). Maltodextrin, pectin and soy protein isolate as carrier agents in the encapsulation of anthocyanins-rich extract from jaboticaba pomace. *Food and Bioproducts Processing, 102*, 186–194. https://doi.org/10.1016/j.fbp.2016.12.012

Pereira, V. A., de Arruda, I. N. Q., & Stefani, R. (2015). Active chitosan/PVA films with anthocyanins from Brassica oleraceae (Red Cabbage) as Time-Temperature Indicators for application in intelligent food packaging. *Food Hydrocolloids, 43*, 180–188. https://doi.org/10.1016/j.foodhyd.2014.05.014

Pourjavaher, S., Almasi, H., Meshkini, S., Pirsa, S., & Parandi, E. (2017). Development of a colorimetric pH indicator based on bacterial cellulose nanofibers and red cabbage (Brassica oleraceae) extract. *Carbohydrate Polymers, 156*, 193–201. https://doi.org/10.1016/j.carbpol.2016.09.027

Prietto, L., Mirapalhete, T. C., Pinto, V. Z., Hoffmann, J. F., Vanier, N. L., Lim, L.-T., … da Rosa Zavareze, E. (2017). pH-sensitive films containing anthocyanins extracted from black bean seed coat and red cabbage. *LWT, 80*, 492–500. https://doi.org/10.1016/j.lwt.2017.03.006

Priyadarshi, R., Roy, S., Ghosh, T., Biswas, D., & Rhim, J.-W. (2021). Antimicrobial nanofillers reinforced biopolymer composite films for active food packaging applications - a review. *Sustainable. Materials and Technologies, e00353*. https://doi.org/10.1016/j.susmat.2021.e00353

Rawdkuen, S., Faseha, A., Benjakul, S., & Kaewprachu, P. (2020). Application of anthocyanin as a color indicator in gelatin films. *Food Bioscience, 36*, Article 100603. https://doi.org/10.1016/j.fbio.2020.100603

Roy, S., Kim, H.-J., & Rhim, J.-W. (2021). Synthesis of Carboxymethyl Cellulose and Agar-Based Multifunctional Films Reinforced with Cellulose Nanocrystals and Shikonin. *ACS Applied Polymer Materials, 3*(2), 1060–1069. https://doi.org/10.1021/acsapm.0c01307

Sakulnarmrat, K., & Konczak, I. (2022). Encapsulation of Melodorum fruticosum Lour. anthocyanin-rich extract and its incorporation into model food. *LWT, 153*, Article 112546. https://doi.org/10.1016/j.lwt.2021.112546

Santos, S. S., Rodrigues, L. M., Costa, S. C., & Madrona, G. S. (2019). Antioxidant compounds from blackberry (Rubus fruticosus) pomace: Microencapsulation by spray-dryer and pH stability evaluation. *Food Packaging and Shelf Life, 20*, Article 100177. https://doi.org/10.1016/j.fpsl.2017.12.001

Saricaoglu, F. T., Tural, S., Gul, O., & Turhan, S. (2018). High pressure homogenization of mechanically deboned chicken meat protein suspensions to improve mechanical and barrier properties of edible films. *Food Hydrocolloids, 84*, 135–145. https://doi.org/10.1016/j.foodhyd.2018.05.058

Sáyago-Ayerdi, S. G., Velázquez-López, C., Montalvo-González, E., & Goñi, I. (2014). By-product from decoction process of Hibiscus sabdariffa L. calyces as a source of polyphenols and dietary fiber. *Journal of the Science of Food and Agriculture, 94*(5), 898–904. https://doi.org/10.1002/jsfa.6333

Sganzerla, W. G., Pereira Ribeiro, C. P., Uliana, N. R., Cassetari Rodrigues, M. B., da Rosa, C. G., Ferrareze, J. P., … Nunes, M. R. (2021). Bioactive and pH-sensitive films based on carboxymethyl cellulose and blackberry (Morus nigra L.) anthocyanin-rich extract: A perspective coating material to improve the shelf life of cherry tomato (Solanum lycopersicum L. var. cerasiforme). *Biocatalysis and Agricultural Biotechnology, 33*, Article 101989. https://doi.org/10.1016/j.bcab.2021.101989

Sharif, N., Khoshnoudi-Nia, S., & Jafari, S. M. (2020). Nano/microencapsulation of anthocyanins; a systematic review and meta-analysis. *Food Research International, 132*, Article 109077. https://doi.org/10.1016/j.foodres.2020.109077

Shi, C., Zhang, J., Jia, Z., Yang, X., & Zhou, Z. (2021). Intelligent <scp>pH</scp> indicator films containing anthocyanins extracted from blueberry peel for monitoring tilapia fillet freshness. *Journal of the Science of Food and Agriculture, 101*(5), 1800–1811. https://doi.org/10.1002/jsfa.10794

Silva-Pereira, M. C., Teixeira, J. A., Pereira-Júnior, V. A., & Stefani, R. (2015). Chitosan/corn starch blend films with extract from Brassica oleraceae (red cabbage) as a visual indicator of fish deterioration. *LWT - Food Science and Technology, 61*(1), 258–262. https://doi.org/10.1016/j.lwt.2014.11.041

Silva, S., Costa, E. M., Calhau, C., Morais, R. M., & Pintado, M. E. (2017). Anthocyanin extraction from plant tissues: A review. *Critical Reviews in Food Science and Nutrition, 57*(14), 3072–3083. https://doi.org/10.1080/10408398.2015.1087963

Singh, S., Nwabor, O. F., Syukri, D. M., & Voravuthikunchai, S. P. (2021). Chitosan-poly (vinyl alcohol) intelligent films fortified with anthocyanins isolated from Clitoria ternatea and Carissa carandas for monitoring beverage freshness. *International Journal of Biological Macromolecules, 182*, 1015–1025. https://doi.org/10.1016/j.ijbiomac.2021.04.027

Singleton, V. L., Orthofer, R., & Lamuela-Raventós, R. M. (1999). [14] Analysis of total phenols and other oxidation substrates and antioxidants by means of folin-ciocalteu reagent (pp. 152–178). https://doi.org/10.1016/S0076-6879(99)99017-1.

Soultani, G., Evageliou, V., Koutelidakis, A. E., Kapsokefalou, M., & Komaitis, M. (2014). The effect of pectin and other constituents on the antioxidant activity of tea. *Food Hydrocolloids, 35*, 727–732. https://doi.org/10.1016/j.foodhyd.2013.08.005

Tarone, A. G., Cazarin, C. B. B., & Marostica Junior, M. R. (2020). Anthocyanins: New techniques and challenges in microencapsulation. *Food Research International, 133*, Article 109092. https://doi.org/10.1016/j.foodres.2020.109092

Teixeira, S. C., Soares, N. de F. F., & Stringheta, P. C. (2021). Desenvolvimento de embalagens inteligentes com alteração colorimétrica incorporadas com antocianinas: uma revisão crítica. *Brazilian Journal of Food Technology*, *24*. https://doi.org/10.1590/1981-6723.03321.

Vasco, C., Ruales, J., & Kamal-Eldin, A. (2008). Total phenolic compounds and antioxidant capacities of major fruits from Ecuador. *Food Chemistry, 111*(4), 816–823. https://doi.org/10.1016/j.foodchem.2008.04.054

Wu, C., Sun, J., Zheng, P., Kang, X., Chen, M., Li, Y., … Pang, J. (2019). Preparation of an intelligent film based on chitosan/oxidized chitin nanocrystals incorporating black rice bran anthocyanins for seafood spoilage monitoring. *Carbohydrate Polymers, 222*, Article 115006. https://doi.org/10.1016/j.carbpol.2019.115006

Wu, L., Zhang, J., & Watanabe, W. (2011). Physical and chemical stability of drug nanoparticles. *Advanced Drug Delivery Reviews, 63*(6), 456–469. https://doi.org/10.1016/j.addr.2011.02.001

Yang, W., Guo, Y., Liu, M., Chen, X., Xiao, X., Wang, S., … Chen, F. (2022). Structure and function of blueberry anthocyanins: A review of recent advances. *Journal of Functional Foods, 88*, Article 104864. https://doi.org/10.1016/j.jff.2021.104864

Yang, Z., Zhai, X., Zou, X., Shi, J., Huang, X., Li, Z., … Xiao, J. (2021). Bilayer pH-sensitive colorimetric films with light-blocking ability and electrochemical writing property: Application in monitoring crucian spoilage in smart packaging. *Food Chemistry, 336*, Article 127634. https://doi.org/10.1016/j.foodchem.2020.127634

Yong, H., Wang, X., Bai, R., Miao, Z., Zhang, X., & Liu, J. (2019). Development of antioxidant and intelligent pH-sensing packaging films by incorporating purple-fleshed sweet potato extract into chitosan matrix. *Food Hydrocolloids, 90*, 216–224. https://doi.org/10.1016/j.foodhyd.2018.12.015

Yu, L. (2001). Amorphous pharmaceutical solids: Preparation, characterization and stabilization. *Advanced Drug Delivery Reviews, 48*(1), 27–42. https://doi.org/10.1016/S0169-409X(01)00098-9

Zabihollahi, N., Alizadeh, A., Almasi, H., Hanifian, S., & Hamishekar, H. (2020). Development and characterization of carboxymethyl cellulose based probiotic nanocomposite film containing cellulose nanofiber and inulin for chicken fillet shelf life extension. *International Journal of Biological Macromolecules, 160*, 409–417. https://doi.org/10.1016/j.ijbiomac.2020.05.066

Zabot, G. L., Silva, E. K., Azevedo, V. M., & Meireles, M. A. A. (2016). Replacing modified starch by inulin as prebiotic encapsulant matrix of lipophilic bioactive compounds. *Food Research International, 85*, 26–35. https://doi.org/10.1016/j.foodres.2016.04.005

Zhai, X., Li, Z., Zhang, J., Shi, J., Zou, X., Huang, X., … Povey, M. (2018). Natural Biomaterial-Based Edible and pH-Sensitive Films Combined with Electrochemical Writing for Intelligent Food Packaging. *Journal of Agricultural and Food Chemistry, 66*(48), 12836–12846. https://doi.org/10.1021/acs.jafc.8b04932

Zhai, X., Shi, J., Zou, X., Wang, S., Jiang, C., Zhang, J., … Holmes, M. (2017). Novel colorimetric films based on starch/polyvinyl alcohol incorporated with roselle anthocyanins for fish freshness monitoring. *Food Hydrocolloids, 69*, 308–317. https://doi.org/10.1016/j.foodhyd.2017.02.014

Zhang, J., Zou, X., Zhai, X., Huang, X., Jiang, C., & Holmes, M. (2019). Preparation of an intelligent pH film based on biodegradable polymers and roselle anthocyanins for monitoring pork freshness. *Food Chemistry, 272*, 306–312. https://doi.org/10.1016/j.foodchem.2018.08.041

Zhang, X., Liu, Y., Yong, H., Qin, Y., Liu, J., & Liu, J. (2019). Development of multifunctional food packaging films based on chitosan, TiO2 nanoparticles and anthocyanin-rich black plum peel extract. *Food Hydrocolloids, 94*, 80–92. https://doi.org/10.1016/j.foodhyd.2019.03.009

Zhen, J., Villani, T. S., Guo, Y., Qi, Y., Chin, K., Pan, M.-H., … Wu, Q. (2016). Phytochemistry, antioxidant capacity, total phenolic content and anti-inflammatory activity of Hibiscus sabdariffa leaves. *Food Chemistry, 190*, 673–680. https://doi.org/10.1016/j.foodchem.2015.06.006

Zheng, Y., Li, X., Huang, Y., Li, H., Chen, L., & Liu, X. (2022). Two colorimetric films based on chitin whiskers and sodium alginate/gelatin incorporated with anthocyanins for monitoring food freshness. *Food Hydrocolloids, 127*, Article 107517. https://doi.org/10.1016/j.foodhyd.2022.107517

Zimeri, J. (2002). The effect of moisture content on the crystallinity and glass transition temperature of inulin. *Carbohydrate Polymers, 48*(3), 299–304. https://doi.org/10.1016/S0144-8617(01)00260-0